**US Army Corps of Engineers**
Construction Engineering Research Laboratory

**USACERL Technical Report 99/40**
**April 1999**

# Evaluation of Surface Preparation and Application Parameters for Arc-Sprayed Metal Coatings

Alfred D. Beitelman

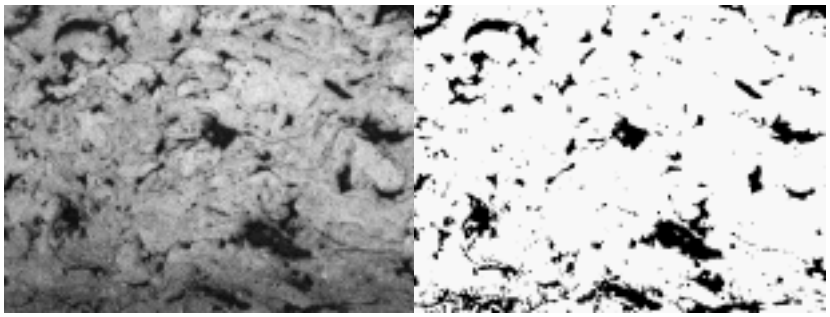

The U.S. Army Corps of Engineers uses an 85:15 zinc:aluminum alloy coating on hydraulic structures exposed to severe environments, such as those areas on a structure subject to impact and abrasion damage caused by ice and floating debris. Properly applied coatings of this type have lasted 8 to 10 years. However, the Corps has experienced premature failure of these systems due to inappropriate surface preparation and application procedures.

Much advancement in metal spray technology has occurred in recent years. Other alloys have been designed for metal spray application. These metals combined with technological advances in application equipment may provide better performance and yield more productive application rates.

Under contract to the U.S. Army Construction Engineering Research Laboratory (CERL), KTA-Tator, Inc., investigated the effects of surface preparation and application parameters on the performance characteristics of 85:15 zinc:aluminum alloy versus four other materials used for metal coating (metallizing) of Corps structures. These attributes were evaluated by using the electric arc process of metallizing.

The effects of surface preparation and application parameters on adhesion, cavitation, and erosion, and porosity and oxide content were investigated, and a statistical analysis of the results was performed. Based upon the results of this study, a list of suggested surface preparation and coating application parameters, as well as minimum tensile adhesion values (based upon use of a pneumatic adhesion tester) was developed for each respective material.

# Executive Summary

Under contract to the U.S. Army Construction Engineering Research Laboratories (CERL), KTA-Tator, Inc. (KTA) investigated the effects of surface preparation and application parameters on the performance characteristics of 85:15 zinc: aluminum (Zn:Al) alloy versus four other metal alloys used for metal coating (metallizing) of Corps structures. These attributes were evaluated by using the electric arc process of metallizing. The performance of 85:15 Zn:Al alloy metal coating was compared to the performance characteristics of 100% Al coating, 100% Zn coating, 85:15 Zn:Al pseudo alloy coating and 90:10 aluminum:aluminum oxide (Al:$AlO_2$) alloy coating. The surface preparation variables included: shallow versus deep surface profile depth (1 and 3 mils, respectively), and surface profile shape (round versus angular). The application parameters investigated included: stand-off distance (spray gun to surface), spray angle, amperage, and atomization air pressure. In each case, the equipment manufacturer's recommended parameter ("center value") was used, as were parameters both lower than that recommended for quality and higher than recommended. These parameters are summarized below.

**Application Parameters**

| Variable | Center Value | High Value | Low Value |
|---|---|---|---|
| Stand-off distance | 12 in. (recommended) | 18 in. (150% of recommended) | 6 in. (50% of recommended) |
| Spray angle* | 90 degrees | 67.5 degrees | 45 degrees |
| Power supply | Recommended amperage for highest quality (375 amps) | Recommended amperage for highest production rate (450 amps) | Below recommended amperage for highest quality (300 amps) |
| Atomization air | Recommended pressure (80 psi) | Higher than recommended pressure (90 psi) | Lower than recommended pressure (70 psi) |
| * The values used for spray angle are not centered around a midpoint value. The highest value of angle (90 degrees) is that used for the default setting. This anomaly is correctly handled in the design matrix described later in Table 4 on page 20. | | | |

The effects of surface preparation and application parameters on adhesion, cavitation and erosion, and porosity and oxide content were investigated, and a statistical analysis of the results was performed. Based upon the results of this study, a list of suggested surface preparation and coating application parameters, as well as minimum tensile adhesion values (based upon use of a pneumatic

adhesion tester) was developed for each respective alloy. These data are summarized below. Practical ranges are indicated in parentheses for the surface preparation and coating application parameters.

***Material 1 – zinc:aluminum alloy (85:15)***

- Angular 3 mil surface profile (3–3.5 mils)
- Distance to the surface of 6 to 10 inches (6–10 inches)
- Angle of the spray gun of 90° (85°–95°)
- Power to the spray gun of 300 amps (275–325 amps)
- Atomization air pressure at the gun of 90 psi (85–95 psi)
- Minimum tensile adhesion value (from Table E7) is 1,000 psi

***Material 2 – 100% aluminum***

- Angular 3 mil surface profile (3–3.5 mils)
- Distance to the surface of 6 to 11 inches (6–11 inches)
- Angle of the spray gun of 90°(85°–95°)
- Power to the spray gun of 450 amps (425–475 amps)
- Atomization air pressure at the gun of 90 psi (85–95 psi)
- Minimum tensile adhesion value (from Table E7) is 1,500 psi

***Material 3 – 100% zinc***

- Angular 3 mil surface profile (3–3.5 mils)
- Distance to the surface of 6 inches (6–8 inches)
- Angle of the spray gun of 90°(85°–95°)
- Power to the spray gun of 400 amps (375–425 amps)
- Atomization air pressure at the gun of 90 psi (85–95 psi)
- Minimum tensile adhesion value (from Table E7) is 750 psi

***Material 4 – zinc:aluminum pseudo alloy (85:15 pseudo)***

- Angular 3 mil surface profile (3–3.5 mils)
- Distance to the surface of 6 inches (6–8 inches)
- Angle of the spray gun of 90°(85°–95°)
- Power to the spray gun of 350-400 amps (350–400 amps)
- Atomization air pressure at the gun of 90 psi (85–95 psi)
- Minimum tensile adhesion value (from Table E7) is 1,250 psi

***Material 5 – aluminum:aluminum oxide alloy (90:10)***

- Angular 3 mil surface profile (3–3.5 mils)
- Distance to the surface of 6-10 inches (6–10 inches)
- Angle of the spray gun of 90°(85°–95°)
- Power to the spray gun of 390 amps (375–425 amps)

- Atomization air pressure at the gun of 80-90 psi (80–90 psi)
- Minimum tensile adhesion value (from Table E7) is 1,675 psi

Finally, KTA is recommending that additional research be conducted in the form of a follow-up study. In the discussion of Taguchi modeling (the experimental design used for this study) beginning on page 27, a four-step diagram is used to describe the process. This study completed three of those steps. CERL is strongly urged to complete the fourth step in which the results are confirmed through re-testing. It is suggested that this additional testing focus on the confirmation of the suggested application conditions to enhance performance and minimize applied coating variation. A well-designed branch experiment in which the default application angle is truly the center-point value in an orthogonal array is also suggested to clarify the role that angle of the gun plays (if any) in determining performance.

The results from this research also suggest that some of the commonly used means to assess coating performance in the field are of doubtful value to a Corps inspector. Specifically, adhesion is a widely used test to determine adequacy of applied thermal spray films. The testing confirms that adhesion will distinguish between a well-prepared surface and a poorly prepared surface. However, adhesion results for thermal spray materials applied under very poor conditions are surprisingly high once surface preparation is optimized. This outcome suggests that adhesion results are not good predictors of physical performance for these materials. As an alternative to using adhesion alone as a measure of applied thermal spray metal integrity, it is suggested a procedure be developed, amenable to field use, which can estimate porosity and oxide content. Finally, the results presented in this report are technical and scientific in nature. It is suggested that a simple guide be developed for specifiers, engineers, and inspectors that presents the significance of these results in layman's terms.

# Foreword

This study was conducted for U.S. Army Corps of Engineers (USACE) under Civil Works Work Unit L18, "HPMS High Performance Paint Systems." The technical monitor was Andy Wu, CECW-EE.

The work was performed by the Materials and Structures Branch (CF-M), Facilities Division (CF), U.S. Army Construction Engineering Research Laboratory (CERL). The CERL Principal Investigator was Alfred D. Beitelman. The major portion of this work was done by KTA-Tator, Inc., of Pittsburgh, PA, under contract DACW88-97-M-073 dated 21 March 1997. Dr. Ilker Adiguzel is Chief, CF-M, and Michael Golish is Division Chief, CF. The CERL technical editor was Linda L. Wheatley, Information Technology Laboratory.

The Director of CERL is Dr. Michael J. O'Connor.

# Contents

# List of Figures and Tables

## Figures



## Tables

# 1 Introduction

## Background

The U.S. Army Corps of Engineers uses an 85:15 zinc:aluminum (Zn:Al) alloy coating on hydraulic structures exposed to severe environments, such as those areas on a structure subject to impact and abrasion damage caused by ice and floating debris. Properly applied coatings of this type have lasted 8 to 10 years. However, the Corps has experienced premature failure of these systems due to inappropriate surface preparation and application procedures.

Much advancement in metal spray technology has occurred in recent years. Other alloys have been designed for metal spray application. These metals combined with technological advances in application equipment may provide better performance and yield more productive application rates.

## Objective

The primary objective of this study was to measure the effects of various surface preparation and application parameters on the performance of 85:15 Zn:Al alloy coating, which is currently used by the Corps. The performance characteristics included porosity and oxide content of the applied coating, erosion or cavitation resistance, and tensile adhesion. Secondarily, these same performance characteristics are compared to other zinc and aluminum containing thermal spray coatings. The results of this research may be used to develop thermal spray process parameters and inspection criteria for Corps of Engineers thermal spray projects.

## Approach

The research effort was categorized by the U.S. Army Construction Engineering Research Laboratory (CERL) according to six major tasks: Task 1, “Experimental Design”; Task 2, “Test Panel Preparation”; Task 3, “Test Coating Application”; Task 4, “Testing of Coatings”; Task 5, “Analytical Modeling of the Thermal Spray Process”; and Task 6, “Statistical Analysis of Results.”

KTA subcontracted the porosity and oxide content evaluation (component of Task 4), the analytical modeling of the thermal spray process (Task 5), and the statistical analysis of the results (Task 6) to the research arm of SSPC, The Society for Protective Coatings, Pittsburgh, PA. The coating application procedures (Task 3) were subcontracted to American Boiler and Chimney (ABC), Neville Island, PA. The actual coating application was conducted at the KTA-Pittsburgh facility using equipment and personnel from KTA, ABC, and TAFA Corporation, Concord, NH.

The experiments included four application variables at each of three parameters for five coating materials using the Taguchi L9 fractional factorial experimental design. The coating materials included Zn:Al (85:15) alloy, aluminum (Al), Zinc (Zn), Zn:Al (85:15) pseudo alloy, and Al:Aluminum Oxide ($AlO_2$) (90:10) alloy. The test specimens were prepared for the evaluation of porosity and oxide content, cavitation/erosion resistance, and tensile adhesion. The project approach is described in more detail in Chapter 2.

## Mode of Technology Transfer

Information from this report was used in the preparation of Corps of Engineers Guide Specification 09971, *Metallizing: Hydraulic Structures*.

## Units of Weight and Measure

U.S. standard units of measure are used throughout this report. A table of conversion factors for Standard International (SI) units is provided below.

| SI conversion factors | | |
|---|---|---|
| 1 in. | = | 2.54 cm |
| 1 psi | = | 6.89 kPa |
| 1 mil | = | 25.4 $\mu$ |
| 1 lb | = | 2.2 kg |

# 2 Description of Major Project Tasks

Following is a description of the major project tasks associated with this research effort. The data generated from each of these major tasks was used in reaching conclusions regarding the thermal spray process.

## Development of Experimental Design

The experiment included four application variables at each of three parameters, for five coating materials. To reduce the number of specimens for the project, a Taguchi L9 fractional factorial experimental design was used. The Taguchi L9 experimental design resulted in 21 experiments for each coating material (9 variables plus 12 center points). The surface preparation variable was held constant. Accordingly, 105 specimens were prepared for the evaluation of porosity and oxide content, cavitation/erosion resistance, and tensile adhesion.

The five materials evaluated in this study were:

Material 1 - Zn:Al (85:15) alloy
Material 2 - Al
Material 3 - Zn
Material 4 - Zn:Al (85:15) pseudo alloy
Material 5 – Al:$AlO_2$ (90:10) alloy.

An additional 20 specimens (4 per coating material) were prepared to evaluate the adhesion characteristics of the 5 metal coatings over 4 surface preparation variables. Each of the four application variables and three parameters used for the five metal coatings are described below.

### *Application Variable 1: Parameters A, B, and C – Stand-off Distance*

The stand-off distance used for application of the five metal coatings included: the equipment manufacturer's recommended distance (12 in.); 50 percent of the recommended distance (6 in.); and 150 percent of the recommended distance (18 in.).

### *Application Variable 2: Parameters A, B, and C – Spray Angle*

The spray angle used for the application of the five metal coatings included: mounting the gun normally to the surface (90 degrees); and at angles of 67.5 degrees to the surface and 45 degrees to the surface.

### *Application Variable 3: Parameters A, B, and C – Amperage*

The amperage used for the application of the five metal coatings included: the level of power recommended by the equipment manufacturer to provide the highest quality of coating film (375 amps); the level of power recommended by the equipment supplier to achieve the highest rate of production (450 amps); and a power level lower than the manufacturer's recommendation for quality application (300 amps).

### *Application Variable 4: Parameters A, B, and C – Atomization Air Pressure*

The atomization air pressure used for the application of the five metal coatings included: the equipment manufacturer's recommended atomization air pressure (80 psi); an atomization air pressure higher than recommended (90 psi), and a pressure lower than recommended (70 psi).

The surface preparation used for the four application variables described above remained constant. Steel surfaces were abrasive blast cleaned to a “white metal” condition (SSPC-SP5/NACE* No. 1) using an aluminum oxide abrasive, and yielding a nominal 3.0 mil surface profile. To observe the effect of surface preparation on coating performance (adhesion), two surface preparation variables were included in the experimental design: abrasive material and surface profile. These variables were independent of the application variables described above. That is, the five metal coatings were applied using the manufacturer's recommended stand-off distance (12 in.), spray angle (90 degrees), amperage (375 amps), and atomization air pressure (80 psi). The surface preparation variables included blast profile shape (angular versus round) and depth (shallow versus deep). Specifically, specimens were abrasive blast cleaned to a “white metal” condition (SSPC-SP5/NACE No. 1) using steel shot to produce a rounded profile at both a nominal 1 mil and a 3 mil surface profile depth. A second set of specimens

* NACE - National Association of Corrosion Engineers

were prepared using an aluminum oxide abrasive to produce an angular profile at both a nominal 1 mil and a 3 mils surface profile depth.

## Preparation of Sample Panels — Thermal Spray Application

Prior to project initiation, a written protocol was developed from the Statement of Work provided by CERL. The protocol was reviewed by CERL and Sulit Engineering. The following two sections describe Task 2 and Task 3, respectively, and are based upon the established protocol. Laboratory data records indicating the variables and conditions for each application are shown in Appendices A through E.

### *Panel Fabrication and Surface Preparation*

Test specimens were fabricated, prepared, and coated at the KTA-Tator, Inc. facilities in Pittsburgh, PA. One hundred twenty-five 3/16 in. x 6 in. x 12 in. test plates were fabricated from American Society for Testing and Materials (ASTM) A36 grade hot-rolled carbon steel. Prior to surface preparation, each specimen was uniquely identified using a three-digit number. The number was stenciled in each of the four corners of each plate, and again in the middle of the plate. The number directly corresponds to the surface preparation, alloy, and application variable for each specimen. Edges of the steel specimens were ground to a slight radius, then the specimens were solvent cleaned in accordance with SSPC-SP1, "Solvent Cleaning." Subsequently, the specimens were abrasive blast cleaned in accordance with SSPC-SP5/NACE No. 1, "White Metal," according to the schedule shown in Table 1.

**Table 1. Abrasive/surface profile parameters.**

| Abrasive | Surface Profile | Number of Specimens |
|---|---|---|
| Aluminum oxide | 1.0 mil average | 5 |
| Aluminum oxide | 3.0 mil average | 110 |
| Steel shot | 1.0 mil average | 5 |
| Steel shot | 3.0 mil average | 5 |

Prior to blast cleaning, the compressed air source was verified for cleanliness from moisture and oil in accordance with ASTM D4285, "Test Method for Indicating Oil or Water in Compressed Air." Optimum blast cleaning nozzle pressure (90–100 psi) was used. Blast pressure was verified using a hypodermic needle pressure gage. Ambient conditions in the blast room, including air and surface temperature, relative humidity, and dew point were measured and recorded prior to blast cleaning. After blast cleaning, surface cleanliness was assessed in accordance with SSPC VIS 1-89, photograph ASP5. Surface profile depth was measured on representative test specimens in accordance with ASTM D4417, method C (replica tape). After surface preparation, the cleanliness of the specimens was preserved by placing them in a forced convection oven maintained at 100 °F, until application was initiated.

### *Thermal Spray Coating Application, Equipment, and Procedure*

All metal spray application equipment and wire were provided by TAFA. All metal spray application was conducted by TAFA and KTA. Two representatives from ABC were also present throughout the application procedures. Prior to metal spray application, the spray room conditions were established. Conditions monitored included: ventilation at the spray booth (feet per minute); air temperature; relative humidity; dew point; surface temperature; and barometric pressure. These conditions were also monitored and recorded throughout the application process. A recording hygrothermograph was used to record the air temperature and relative humidity throughout the project, 24 h/day.

The metal spray application was performed using the TAFA Model 8860 High Amperage Thermal Spray System with an automated spray gun mounted to the arm of the KTA semi-automatic hydraulically operated spray arm, using a custom designed mounting bracket. The spray arm traversed the spray gun horizontally at a predetermined rate of speed. A custom designed magnetic plate holder permitted the plate to be positioned at varying distances (in 3-in. segments) from the spray gun tip, and was equipped to rotate the plate 90 degrees for cross hatch application of the metal spray. All application was conducted using a 50 percent overlap technique, with successive coating layers applied at right angles (cross-hatch). The equipment was capable of continuously spraying each material for a minimum of 15 minutes without sputtering or shorting. All application was conducted using 1/8-in. diameter wire. The metal alloys and the target metal coating thickness data are described in Table 2.

**Table 2. Metal spray target thicknesses.**

| Coating Material | Thickness |
|---|---|
| 85:15 Zn:Al Alloy | 16 +/- 2 mil |
| Aluminum | 10 +/- 2 mil |
| Zinc | 16 +/- 2 mil |
| 85:15 Zn:Al Pseudo | 16 +/- 2 mil |
| 90:10 Al/$AlO_2$ Alloy | 10 +/- 2 mil |

Coating thickness was measured non-destructively using a PosiTector Model 6000 F1 electromagnetic coating thickness gage calibrated before and after each use using National Institute of Standards and Technology (NIST) calibration plates. A magnetic base was measured and subtracted from the total coating thickness to obtain the thickness of the metal coating above the peaks of the profile. Five spot measurements (the average of three gage readings per spot) were obtained. The average of the five spot readings complied with the specified thickness ranges indicated in Table 2. Actual thickness data are contained in Appendix A.

### *Application Variable*

As stated earlier, four application variables were included in the testing protocol. These application variables included: stand-off distance, spray angle, amperage, and atomization air pressure. Specifically, the parameters listed in Table 3 were included in the study.

**Table 3. Application parameters.**

| Variable | Center Value | High Value | Low Value |
|---|---|---|---|
| Stand-off distance | 12 in. (recommended) | 18 in. (150% of recommended) | 6 in. (50% of recommended) |
| Spray angle* | 90 degrees | 67.5 degrees | 45 degrees |
| Power supply | Recommended amperage for highest quality (375 amps) | Recommended amperage for highest production rate (450 amps) | Below recommended amperage for highest quality (300 amps) |
| Atomization air | Recommended pressure (80 psi) | Higher than recommended pressure (90 psi) | Lower than recommended pressure (70 psi) |
| * The values used for spray angle are not centered around a midpoint value. The highest value of angle (90 degrees) is that used for the default setting. This anomaly is correctly handled in the design matrix described in Table 4. | | | |

The processes used to control each of the project variables are described below. The stand-off distance was adjusted by repositioning the specimen holder a specific distance from the spray nozzle. For example, when the recommended distance was 12 in., representative specimens were sprayed at 6 in. (50 percent), 12 in. (recommended), and 18 in. (150 percent). The actual distance was measured and recorded.

The spray angle was adjusted with the aid of a variable angle combination square equipped with a protractor and an 18-in. blade. The blade holder was positioned perpendicularly on the vertical specimen surface. The blade was adjusted as required so that the spray gun nozzle was either at 90 degrees to the surface, 67.5 degrees to the surface, or 45 degrees to the surface. The angle was adjusted in combination with the stand-off distances described above.

The power supply was adjusted by selecting the amperages recommended for the highest quality of application (375 amps); the highest production rate (450 amps); and a level below the recommended power for a high quality coating (300 amps). The actual amperage setting used for each of the three parameters was recorded.

The atomization air pressure was adjusted by setting the pressure regulator at the manufacturer's suggested pressure (80 psi); a pressure higher than that recommended by the manufacturer (90 psi); and a pressure lower than that recommended by the manufacturer (70 psi). The actual atomization pressure setting used for each of the three parameters was recorded.

The manufacturer's recommended spray rates were observed as listed in Table 4. All coating materials were supplied by TAFA, Inc., through ABC Co.

**Table 4. Application rates for metal spray materials.**

| Coating Material | Spray Rate |
|---|---|
| 85:15 Zn:Al Alloy | 21 lb of wire/h/100 amp |
| Aluminum | 8 lb of wire/h/100 amp |
| Zinc | 21 lb of wire/h/100 amp |
| 85:15 Zn:Al Pseudo | 14 lb of wire/h/100 amp |
| 90:10 Al:$AlO_2$ Alloy | 8 lb of wire/h/100 amp |

### *Sample Preparation Results*

Except for the Al:$AlO_2$ (90:10) samples (material 5), preparation activities were uneventful. Material 5 showed noticeable "burning" in the plasma, which is consistent with the higher incidence of black inclusions, visible to the naked eye, in samples of material 5.

## Physical Testing of Specimens

The coated specimens were subjected to three test procedures. The results of the testing were used to perform a statistical analysis of the effect of the application variables and parameters on coating performance. The three tests included erosion resistance (ASTM G32, "Standard Test Method for Cavitation Erosion Using Vibratory Apparatus," modified); coating adhesion (ASTM D4541, "Standard Test Method for Evaluating the Pull Off Strength of Coatings Using Portable Adhesion Testers"); and image analysis and quantification to measure porosity and oxide content. Each of these procedures is described below. Sample preparation prior to testing is also described.

### *Sample Preparation for Testing*

The 3/16 in. x 6 in. x 12 in. coated steel test panels were too large for the porosity/oxide content and erosion resistance testing. Therefore, representative specimens from each of the larger samples were obtained. A band saw equipped with a metal cutting blade was used to cut specimens from each of the four corners of the larger samples. No lubricants or coolants were used during the cutting process. Triplicate samples (1/2 in. x 1/2 in. x 3/16 in.) were removed from each test panel for the erosion resistance testing. A single sample (1/2 in. x 1 in. x 3/16 in.) was removed from each coated panel for the porosity and oxide content evaluation (multiple determinations were made from the single sample). The remaining coated surface area of each panel was used to conduct tensile adhesion testing.

### *Adhesion Testing*

Coating adhesion was conducted in accordance with the procedures set forth in ASTM D4541. A Pneumatic Adhesion Tensile Testing Instrument (PATTI) Model 2A was used, as requested by CERL. Five threaded aluminum pull stubs (previously scarified by abrasive blasting) were attached to each coated test panel using a two component epoxy adhesive (Hysol 907). Accordingly, a total of 625 pull stubs were adhered. Immediately after attaching each pull stub, small diameter,

plastic “cut-off rings” were positioned around the perimeter of the base of the pull stubs to displace any excess adhesive. The cut-off rings were removed after the adhesive was cured, and before adhesion testing began.

Three pistons were used in conjunction with the pneumatic adhesion tester, depending upon the relative adhesion values anticipated. An F-2 piston (0-1,000 psi), an F-4 piston (0-2,000 psi), and an F-8 piston (0-4,000 psi) were used. The piston burst pressure was converted to actual pounds per square inch using a conversion chart corresponding to the piston model. The pull-off tensile adhesion strength readings (psi) for each of the five materials tested are shown in Appendix B.

### *Erosion Resistance Testing*

The technique used to determine the cavitation/erosion resistance of the metal coatings was similar to that described by Schwetzke and Kreye (1996). Their method, in turn, is based upon ASTM G32, “Standard Test Method for Cavitation Erosion Using Vibratory Apparatus.”

The test method involved using 1/2 in. x 1/2 in. x 3/16 in. metallized steel coupons, cut from the larger 6 in. x 12 in. x 3/16 in. specimens. The coated steel coupons were placed in a holder slightly larger than the coupon dimensions, and held in place by set screws. The apparatus holding the test coupon was immersed in a 1,000 milliliter (mL) glass beaker containing deionized water at approximately 22 to 27 °C. The beaker containing deionized water was placed on a lab jack, so that the height of the coupon in relation to the probe tip could be adjusted.

The ultrasonic probe used for the experiment was a Sonics and Materials, Inc. Model VC-501, equipped with a 500 Watt probe, oscillating at a frequency of 20 kiloHertz. The amplitude of the oscillation was adjusted to achieve a value of 62 microns peak-to-peak displacement. The distance between the probe tip and the specimen surface was adjusted to approximately 0.5 cm. The specimen test surface was immersed in the deionized water approximately 12 mm. The diameter of the horn tip was 0.5 in.

The probe was operated in a continuous mode for a period of 15 minutes per specimen. Testing was performed using triplicate specimens. The metallized steel coupons were weighed both before and after testing in order to determine the weight loss (in milligrams) due to cavitation erosion.

Weight loss measurements suffered by three replicate specimens from each coupon in cavitation/erosion are shown in Appendix C.

### *Image Analysis*

#### Description of Technique

Image analysis was performed on metallographic specimens of each of the five thermal spray materials applied to carbon steel plate. The goal of the image analysis was to measure the porosity and oxide content of the thermal spray coatings using Differential Interference Contrast (DIC) microscopy. This method is also known as the Nomarski technique. Under special conditions of lighting and sample exposure, coherent thermal spray metal will have a uniform gray color. Pores and oxide inclusions show up as darker areas.

To prepare samples for viewing, they were first mounted and polished as metallographic specimens. Image acquisition was done using a research grade metallographic microscope. Mounted specimens were viewed using a Charged Coupled Device (CCD) video camera. The images were captured on a computer hard disk directly from the CCD camera as Tagged Image Format (TIF) files.

Image analysis was done using scientific image analysis software (NIHImage, National Institutes of Health, Bethesda, MD). The analysis used a technique called thresholding, followed by binary conversion. This technique segregates the image into its metallic (white) and nonmetallic (black) pore and oxide components. Simple arithmetic is then used to determine the proportion of the surface area, viewed in the image, containing pore and oxide components.

#### Sample Preparation

The protocol used for sample preparation prior to image analysis fell into four phases: cleaning, mounting, polishing, and specimen labeling. Each of these phases is described below.

***Phase 1 (cleaning)***. Samples were 1 in. x 1/2 in. sections of 3/16-in. thick coated steel plate. These had been cut from the original thermal spray samples using a mechanical saw. One hundred and five samples were provided, 1 for each of the Taguchi L9 matrix elements and their 12 center-point specimens for each of the 5 thermal spray alloys. All samples were at least 1/2-in. in from the plate edges. Cut edges on the specimens were deburred using dry 60 grit silicon carbide paper. The uncoated side of each sample was carefully wiped with an ethanol soaked towel to remove any ink from the sample code, without contaminating

the coating. Samples were then subjected to a flowing ethanol rinse, a 30-second ultrasonic treatment immersed in ethanol, and a final rinse in acetone. This rinsing process was followed by a 1 hour bake-out to free the sample of solvent. Sample bake-out was conducted at 80 °C. The sample code was then rewritten on the uncoated side of the specimen.

***Phase 2 (mounting)***. Sample cross-sections were mounted in a two-part epoxy resin (LECO Epoxide), with three sections per circular mount. A vacuum infiltration technique was used to ensure good penetration of coating pores by the mounting medium. Molds were placed in a vacuum chamber, evacuated prior to filling the mold with epoxy. Mounts were cured for 24 hours while standing in water to optimize the integrity of the epoxy.

***Phase 3 (polishing)***. The metallographic mounts were polished using automatic equipment, which handled six mounts at one time. The following sequence of silicon carbide papers was used to polish the samples: 60, 120, 220, 320, 500, 800, 1000, 1200, 2400, 4000. Mounts received a brief 10-second ultrasonic cleaning between each of these polishing steps. The final polishing sequence involved 3 µm and 1 µm diamond, then 0.05 µm aluminum oxide polishing media. Samples were not etched.

***Phase 4 (specimen labeling)***. Samples were mounted in consecutive numerical order. Coated surfaces faced away from the sample with the lowest number in any given mount. Sample numbers were scribed on the top and side of the mount. The sample ID written in ink on the lowest numbered sample in any mount was visible through the clear epoxy resin.

#### Image Acquisition

Image acquisition was done using a research grade metallographic microscope equipped with a Sony grayscale CCD camera. Vernier screws permitted precise lateral and longitudinal sample positioning. The microscope was equipped with optical accessories to permit viewing of specimens using the DIC method. All specimen images were acquired while using this technique. Specimens were always viewed at 200X magnification. The DIC procedure yields images in which oxide, nonmetallic inclusions, and void areas appear darker compared to the bright, polished appearance of the surrounding metal.

Three images were acquired from each mounted specimen. Care was taken to avoid acquiring images from the edges of any specimen. The three sampled areas from each specimen were chosen randomly. Image viewpoints for sampling were chosen by moving the specimen laterally across the field of view using the

vernier screw. Initial focusing of the specimen image was done using the microscope eyepiece. Fine focusing was done to optimize the image seen via the CCD camera. Video output from the CCD camera was viewed at a computer workstation fitted with a video capture board. The capture board was optimized to work with the NIHImage image acquisition and analysis software. A capture function in NIHImage was used to store sampled images onto a hard disk directly from the CCD camera as TIF files. All image capture work was performed at the metallurgical laboratories of Carnegie Mellon University by SSPC research staff.

### Quantification

Analysis was performed on the captured images in SSPC facilities. NIHImage was the software used to perform image analysis and quantification. The analysis began with the thresholding technique. A threshold is a limiting value in the viewed grayscale spectrum. To determine the optimum value for the threshold, inspection of the grayscale values from a large number of positions in representative images in each material batch was required. The range of the grayscale spectrum covers values from 0 (pure white), to 255 (pure black). Placing a cursor over a position in the image that was unoccupied by thermal spray metal or was occupied by an oxide inclusion provided a range of grayscale values suitable for thresholding. These values were always much higher than the grayscale values for the thermal spray alloy metal. The difference in values is obvious in Figure 1. For most specimens, coherent thermal spray metal layers were found to have grayscale values from 0 to 100 in a grayscale spectrum with 256 available values; oxide and pore areas showed grayscale values above 180. These findings suggested that thresholding at a grayscale value of 176 would work well to provide contrast between the metallic and nonmetallic regions of most images.

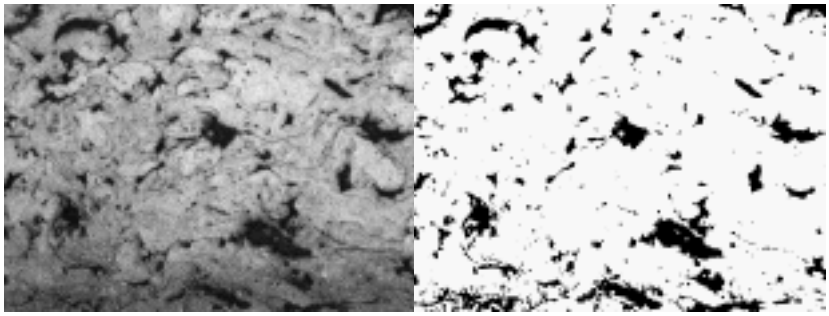

*Initial Image* *Binary converted image*

**Figure 1. Typical image analysis input and output for material 1 (85:15 Zn:Al).**

After thresholding, areas with grayscale values different from the range occupied by metallic layers show as black pixels. All images were then converted to binary form (in which any image pixels below the threshold value are converted to white pixels). This technique segregates the image into its metallic and nonmetallic (pore and oxide) components shown as white and black areas. The converted file was saved with a new name to preserve the original acquired image. The effectiveness of the image analysis method was evaluated by comparison of the original image with its thresholded and binary-converted counterpart.

Simple arithmetic was used to determine the ratio of oxide and porosity in each sample. NIHImage computes the total number of pixels (P) in the image and the subtotal of these pixels that are black (B). The proportion of the surface area, viewed in the image, containing pore and oxide components, is given by B/P. The result is given as a proportion of the total viewed surface area.

The complete results from this analysis and quantification are shown in Appendix D. Figure 1 is typical of the type of images acquired, along with its analyzed counterpart. To the right is the original grayscale TIF image acquired with the CCD camera. To the left is the image after thresholding and binary conversion. The black areas correspond to the locations of oxide and porosity in the sample image. The areal proportion of black pixels is indicative of the porosity and oxide content of the sample.

#### Results

Porosity and oxide content readings for all materials are shown in Appendix D.

#### Problems in Analyzing Aluminum:Aluminum Oxide (90:10)

A subset of the images did not respond well to the proposed threshold level. The majority of the affected specimens were coated with material 5, Al:$AlO_2$ (90:10) alloy. The problem encountered with these specimens was caused by lower film thickness (10 mils versus 16 mils) along with poor applied film quality, resulting in a slightly different approach to image quantification. The difficulty encountered was that of finding a suitable region of the image to quantify. Though the poor film quality is probably typical for this material, the larger concentrations of oxide derived from the alloy provided no difficulty during quantification. The problem is illustrated by Figure 2, which shows the high degree of irregularity in the thermal spray layer for material 5. Alongside the original acquired image is the region accepted for quantification. The quality of definition between metal and pore/oxide in these images is poorer than shown in the preceding figure (typical of the vast majority of specimens from all other materials). Some images

acquired from specimens coated with other metals also showed diminished definition between metal and pore/oxide areas. The majority of these specimens had been prepared with application at unusual angles of incidence (45 degrees). These images all responded well to thresholding at a higher level of 185.

## Taguchi Modeling

### *General*

Taguchi modeling provides a structured approach to solving problems of process improvement. Figure 3 summarizes the Taguchi approach. The modeling exercise hinges on a well-designed experimental matrix, which belongs to a class of designs called orthogonal matrices. The current study was based on a Taguchi L9 matrix, which, by definition, has only three levels for four independent variables. These independent variables are the application parameters shown earlier in Table 3.

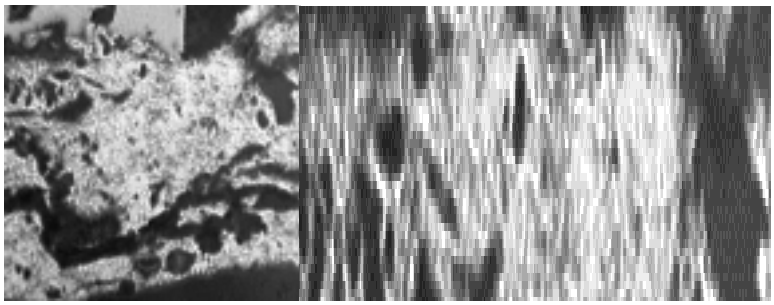

**Figure 2. Typical images from material 5 (Al:$AlO_2$ 90:10).**

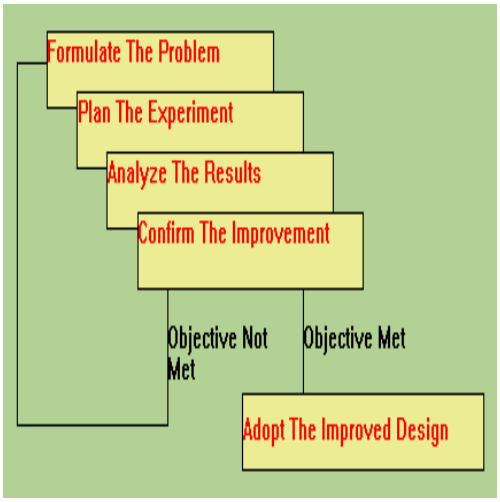


**Figure 3. General description of Taguchi approach to process improvement.**

The overall design also includes an added "outer array" of 12 specimens. As explained below, this design dictated the way modeling exercises were performed. Modeling was done by statistical analysis of the results from the testing described beginning on page 19. There were two core steps to this statistical analysis. The first was an analysis of means (ANOM). This gave graphical information about which of the application parameters had a heavy influence in deciding a performance characteristic (such as adhesion). The second step was to develop a model that measured (quantified) the role of each application parameter. This model takes the form of an equation. The two ways to meet this need are to use analysis of variance (ANOVA), or multiple linear regression. Both approaches are equally valid. Multiple linear regression was used in this research because it not only provided the expected optimizing of application for performance, but also gave information on means to minimize variation in applied film performance. Also, the ANOVA modeling step was not well suited to non-orthogonal arrays, while the multiple linear regression method permitted modeling of both the L9 array and the full set of 21 specimens.

Test results from the 12 outer array specimens were also used to provide an estimate of the precision associated with the default application conditions for each material. This estimate was done, as defined in ASTM E691, "Practice for Conducting an Interlaboratory Study to Determine the Precision of a Test Method," by examining the standard deviations of the results for the 12 samples. In summary, the Taguchi modeling exercise should provide a structured approach to finding the best way to apply each material while ensuring that variations in quality are reduced.

The process of setting up a Taguchi model requires four general steps when used to provide in-plant process improvement. In this study, only the first three steps were requested. The four general steps are:

Step 1: Formulate the problem
Step 2: Plan the experiment
Step 3: Analyze the results
Step 4: Confirm the experiment.

### *Formulating the Problem*

The general problem addressed in this study is the determination of optimum application conditions for five different thermal spray materials. A second exercise involves determining the best performing material of the five, based on acceptance criteria suggested by analysis of key performance characteristics. A

third exercise entails determining the consequences of improper equipment set-up or application technique, and the effect on coating performance.

The general problem is best stated as:

> *For each of five different thermal spray alloys, which set of application conditions provides the best overall performance?*

The second problem is best stated as:

> *Which of the five thermal spray materials gives the best overall performance?*

The third problem is best stated as:

> *For each of the five different thermal spray alloys, which set(s) of application conditions adversely affects overall coating performance?*

To help in formulating the planned response to solving these problems, a process of problem definition was undertaken. This involved the following steps:

- Determine the performance characteristics to be measured.
- List the design variables that affect the product/process response and classify these variables as either controllable parameters (design variables) or noise variables. All of the application parameters are initially believed to be design variables.
- List pairs of application parameters with interactions that may potentially affect the characteristics of a product/process.
- Decide on a tentative number of settings for each application parameter. Three levels were chosen for all application parameters, which ensures that non-monotonic response behavior will be detected.

The performance characteristics to be measured were the thermal spray coating porosity and oxide content, cavitation-erosion resistance, and adhesion to the substrate. Main design variables believed to be important to film quality and film performance were (1) distance from the gun to the surface, (2) angle of gun to the surface, (3) power applied to the gun, and (4) pressure used during application. Additional variables of specific importance to adhesion characteristics were the shape and depth of the profile on the metal surface, dictated by the shape and size of the abrasive used to prepare metal samples.

The pairs of control parameters with interactions that were expected to dictate film formation quality include (1) distance and angle to surface, (2) pressure and power at the gun, and (3) angle to surface and pressure at the gun. Three settings were required for each of the main design variables. The levels used for the main and additional design parameters were described on page 13.

### *Planning the Experiment*

Based on the needs for a design with three levels in each of the four application variables, a Taguchi L9 model was chosen. This model design was extended to include 12 "center" points. This model design results in a total of 21 separate specimen preparation conditions for each of the five thermal spray metal alloys. The center points suggested are in fact "off-center"; the parameter level for angle to the surface is the highest angle (90 degrees) in the design rather than the center of the three levels. All other parameters are set at the true midpoint of the design. The general design used for each set of 21 samples is shown in Table 5.

A separate design assessed the influence of abrasive type and surface profile depth on the adhesion of thermal spray metal to the surface. The design was a two level full-factorial for each of the five thermal spray metal alloys. Four such samples were prepared for each metal alloy. This design, shown in Table 6, assumes that optimum conditions for application prevail with the center-point settings for distance, gun angle, power, and pressure.

**Table 5. Typical Taguchi L9 design with 12 center points.**

| Levels in Design | | | | Values for Each Level | | | |
|---|---|---|---|---|---|---|---|
| Distance | Angle | Power | Pressure | Distance (In.) | Angle (degrees) | Power (amps) | Pressure (psi) |
| -1 | -1 | -1 | -1 | 6 | 45 | 300 | 70 |
| -1 | 1 | 0 | 0 | 6 | 90 | 375 | 80 |
| -1 | 0 | 1 | 1 | 6 | 67.5 | 450 | 90 |
| 0 | -1 | 0 | 1 | 12 | 45 | 375 | 90 |
| 0 | 1 | 1 | -1 | 12 | 90 | 450 | 70 |
| 0 | 0 | -1 | 0 | 12 | 67.5 | 300 | 80 |
| 1 | -1 | 1 | 0 | 18 | 45 | 450 | 80 |
| 1 | 1 | -1 | 1 | 18 | 90 | 300 | 90 |
| 1 | 0 | 0 | -1 | 18 | 67.5 | 375 | 70 |
| 0 | 1 | 0 | 0 | 12 | 90 | 375 | 80 |

Note: The parameters in the last row are repeated 11 more times to make a 12-specimen "outer array."

**Table 6. Design for influence of abrasive and surface profile on adhesion.**

| Abrasive Used | Profile Achieved (mils) | Distance (In.) | Angle (degrees) | Power (amps) | Pressure (psi) |
|---|---|---|---|---|---|
| Aluminum Oxide | 1.0 | 12 | 90 | 375 | 80 |
| Aluminum Oxide | 3.0 | 12 | 90 | 375 | 80 |
| Steel Shot | 1.0 | 12 | 90 | 375 | 80 |
| Steel Shot | 3.0 | 12 | 90 | 375 | 80 |

### *Procedures for Analyzing the Results*

The results placed in the extended L9 matrix were analyzed using software tailored for Taguchi modeling. This software functions as an add-in to Microsoft Excel®. The analysis assessed the influence of application parameters on the following performance characteristics: observed adhesion values, calculated porosity and oxide content, and resistance to cavitation/erosion. The process uses two steps: Analysis of Means (ANOM) and multiple linear regression. The ANOM is only performed on the nine samples from the L9 matrix. Separate multiple linear regression models were created for both the L9 matrix and the complete set of 21 specimens.

These exercises created two types of models, labeled “Y” and “S.” The Y model provides information about how well a thermal spray material performs following application. For example, the Y models for adhesion tell how strong the adhesion will be. The S model gives information on how reproducible this behavior is from sample to sample (it provides information about the standard deviation in expected performance).

Each type of model can be optimized. Y models are typically optimized to maximize desirable performance characteristics. For example, the Y model for adhesion was optimized for maximum adhesion pull-off strength. Other performance characteristics were modeled to reduce Y to limit erosion weight loss and to limit porosity and oxide content. All S models are optimized to minimize standard deviations. The combined results give information on application settings that can enhance coating performance while reducing variation. These application settings may not be the same for each material, nor are they guaranteed to be identical for all measured performance characteristics. To determine the inherent precision of the application method the outer array of 12 specimens was analyzed to determine the standard deviation of the results of all tests. Analysis of the adhesion subset was done separately, using ANOVA.

No other data were required for the base models used in the study. Sorting of the data matched its order with the Taguchi L9 matrix. While image analysis and cavitation/erosion data had three replicates, all adhesion data had five replications. Care was taken to eliminate outlying data points from the analysis and modeling efforts. Data points for adhesion from five of the cavitation erosion outer array specimens of material 5 were eliminated.

## *Examples of Taguchi Analysis*

### Analysis of Means

The ANOM is one technique used in analysis of a Taguchi matrix. This analysis measures the effects of the application parameters on thermal spray performance characteristics. A graphical presentation is typical for these results as seen in Figure 4, for material 1 adhesion. The mean value for each of the three levels is plotted for each of the four application parameters. The slope of the lines joining these three points helps in assessing which parameter is most influential on adhesion. In Figure 4, it is clear that distance from the surface is the most influential application parameter. In a case where highest performance is sought, one can also assess which set of application conditions (for the most influential parameters) will improve performance. Based on Figure 4, a closer distance to the surface (6 in.) results in the greatest adhesion. The other factors do influence material 1 adhesion, but to a far less significant extent.

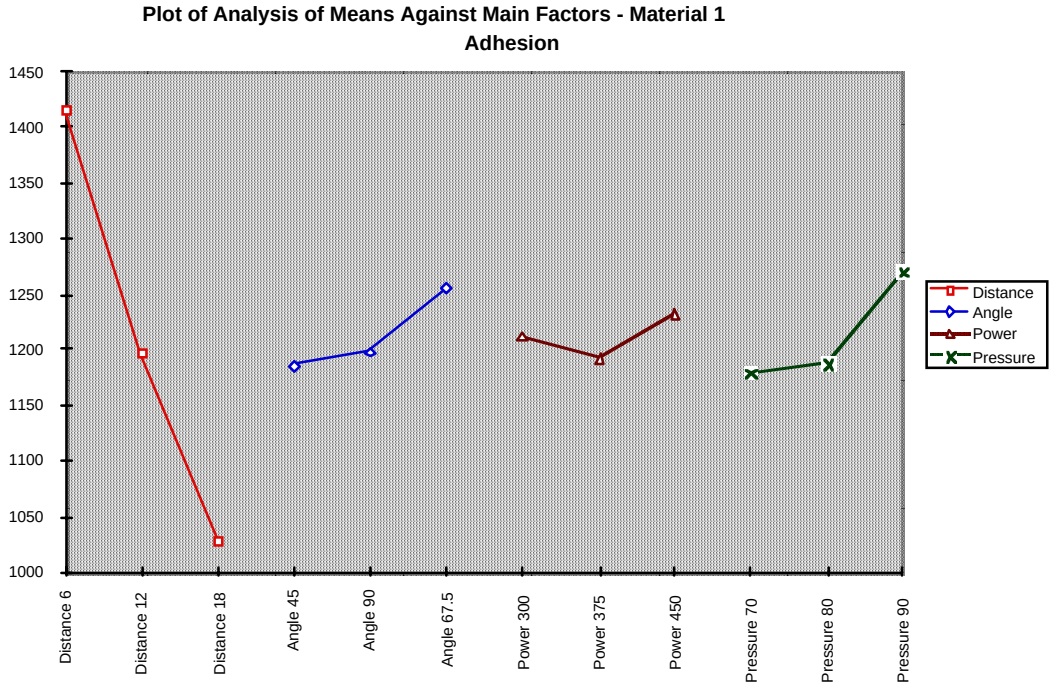


**Figure 4. Typical plot for ANOM material 1 (adhesion results).**

### Analysis of Y and S Tables

Additional outputs from the Taguchi model are the regression/ANOVA tables for the Y and S models. The Y model allows one to determine the best combination of application parameters to optimize performance characteristics. The S model allows one to determine the best combination of parameters to reduce deviation from an expected value. An example for a Y model is described below.

Table 7 is based on a modeling of the image analysis results from the nine samples in the Taguchi L9 array, coated with the Zn:Al (85:15) alloy. Factors are listed in the first column; these are the design variables of the application parameters. Also in this column are the constants associated with the model equation, and self-pairings of primary interactions (AA is distance to distance and so on). The second column includes the coefficients used in a linear equation to express the degree of influence of a variable factor on coating performance (see Equation 1). The third column contains p coefficients from student t-tests of each application parameter against the performance characteristic being measured. The fourth column contains a test of tolerance (how close to an ideal matrix design the levels used for application really are). These are not used in this analysis. The next column reports optimum application settings for achieving high performance. In the last column, an "X" shows that the factor is being used in the model. The bottom portion of Table 7 includes standard multiple regression output such as the R squared values for the regression, the standard error associated with the model and the significance factors for the model (F and Sig F). Where Sig F is less than 0.05, the model is deemed statistically significant.

**Table 7. Y model output for porosity/oxide for Zn:Al (85:15).**

| Factor | Coefficient | P(2 Tail) | Tolerance | Settings | Active |
|---|---|---|---|---|---|
| Constant | 0.1078 | 0.0000 | | | |
| Distance | 0.0261 | 0.0004 | 1 | 6 | X |
| Angle | -0.0267 | 0.0004 | 1 | 45 | X |
| Power | 0.0144 | 0.0286 | 1 | 300 | X |
| Pressure | -0.0028 | 0.6526 | 1 | 70 | X |
| AA | -0.0117 | 0.2817 | 1 | | X |
| BB | 0.0167 | 0.1303 | 1 | | X |
| CC | -0.0067 | 0.5339 | 1 | | X |
| DD | -0.0150 | 0.1707 | 1 | | X |
| $r^2$ | 0.7348 | | | | |
| Adj $r^2$ | 0.6170 | | | | |
| Std Error | 0.0257 | | | | |
| F | 6.2346 | | PRED Y | 0.08 | |
| Sig F | 0.0006 | | EXPERT Y | 0.03 | |

If the performance of the material fits a multiple linear regression model, then the model equation used has the following general form:

**Equation 1 - General Multiple Linear Regression Equation**

$$Y = C+B_1*X_1+B_2*X_2+B_3*X_3+B_4*X_4+B_5*X_5+ \text{(second-order [squared] terms)} + E \text{ (Error Term)}$$

Or, using the labels from Table 7:

**Equation 2 - Multiple Linear Regression With Table Labels**

$$\text{Porosity and Oxide Level (Y)} = \text{Constant}+\text{Distance}*B_1+\text{Angle}*B_2+\text{Power}*B_3 +\text{Pressure}*B_4+ \text{(second-order [squared] terms, AA}*B_5\text{, etc.)}$$

Values for the coefficients $B_n$ are taken directly from Table 7. Values for $X_1$, $X_2$, etc. are -1 because this is the level of the experimental parameter from Table 5 (e.g., distance of 6 in. is level -1 for distance). The result given in the cell to the right of "PRED Y" is based on the levels for Distance, Angle, etc., shown under the "Settings" column. Substituting these values into the above equation for all active terms gives the following:

**Equation 3 - Multiple Linear Regression With Table 7 Values to Predict Porosity and Oxide Content**

$$\text{Porosity and Oxide Level} = 0.1078 + (-1*0.0261) + (-1*-0.0267) + (-1*0.0144) + (-1*-0.0028) + (-0.0117)*(-1)\text{^}2 + 0.0167*(-1)\text{^}2 + (-0.0067)*(-1)\text{^}2 + (-0.0150)*(-1)\text{^}2$$

This calculation yields an exact match with the predicted value for these settings, shown in Table 7, of Y=0.08. No error term is used in this calculation.

The modeling software also allowed calculation of Y when optimum application settings were used. For porosity and erosion weight loss we sought to find the settings that minimized Y. For adhesion, settings to maximize Y were sought. The only value in Table 7 that changes when seeking optimized settings for minimum porosity is that for the angle of application. This variable takes on a new value of 85.5 degrees. The predicted value for Y with these optimized settings is given by the following equation.

**Equation 4 - Multiple Linear Regression to Minimize Porosity and Oxide Content**

*Porosity and Oxide Level = 0.1078 + (-1*0.0261) + (1*(85.5/67.5)*-0.0267) + (-1*0.0144) + (-1*-0.0028) + (-0.0117)*(-1)^2 + 0.0167*(1*(85.5/67.5))^2 + (-0.0067)*(-1)^2 + (-0.0150)*(-1)^2*

This equation yields the optimized value for porosity and oxide content of 0.03, as shown adjacent to the cell labeled "EXPERT Y" in Table 7.

### Y Surface Plot

A visually striking output of the model is the surface plot of the relationship of one design factor against another. For example, Figure 5 shows distance vs. angle and its effect on image porosity. These relationships are also shown as an interaction plot, which illustrates the behavior of the model at levels among those in the experimental design. A three-dimensional interaction plot is also provided along with a straight two-dimensional contour plot. A contour plot is really a bird's-eye view of the surface plot.

The interpretation of these model outputs is provided in Chapter 3.

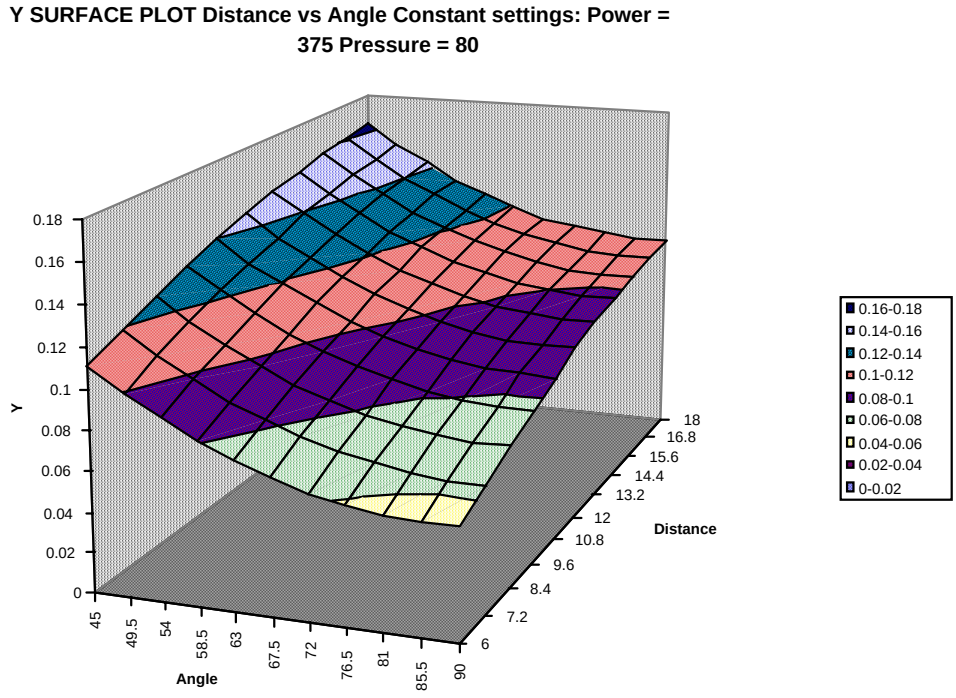


**Figure 5. Typical figure for influence of distance and angle on sample porosity.**

## Statistical Analysis of Results

A series of standard statistical tests was done to analyze the results from the various tests of thermal spray film performance and physical characteristics. Statistical analysis performed included the following:

- Variance for 12 replicates in “center” points of the Taguchi model
- ANOVA to study the effect of abrasive and profile on adhesion
- Regression and correlation analysis.

Regression analysis was done for pairings of dependent and independent variables. The pairings of design factors and performance or physical characteristic responses subjected to regression analysis are given later in Table 21. Simple correlation was also done between ordered pairs of results from the performance characteristics. This correlation is useful in illustrating whether one characteristic (like porosity) has an influence on another (e.g., erosion resistance). The results from this regression analysis are discussed in Chapter 3.

# 3 Analysis of Results

## Taguchi Modeling Results

The most important results from the Taguchi modeling exercise are the p coefficients, the coefficients expressing the influence of factors on performance, and the suggested operating settings to optimize the performance characteristic being observed. These results give insight on the influence that each application parameter has on coating performance. Moreover, the modeling exercise provided useful insights on the influence of combinations of these parameters.

### *Influence of Application Parameters on Adhesion Results*

Table 8 shows the results for the Multiple Linear Regression Analysis of the L9 matrix for adhesion.

**Table 8. Predicted adhesion, degree of factor influence and probability coefficients from Taguchi modeling of adhesion results (L9 matrix only).**

| | Material 1 Zn:Al (85:15) | Material 2 Aluminum | Material 3 Zinc | Material 4 Zn:Al (85:15) Pseudo | Material 5 Al:$AlO_2$ (90:10) |
|---|---|---|---|---|---|
| ***Coefficients of influence on the regression equation*** | | | | | |
| Distance | -194.6 | -15.0 | -169.83 | -114.4 | -81.7 |
| Angle | 1.32 | -94.7 | 10.19 | 15.7 | -118.4 |
| Power | 10.91 | 300.7 | 13.58 | 32.1 | 107.5 |
| Pressure | 46.19 | -41.3 | 43.52 | 11.1 | 4.0 |
| ***Probability Coefficients P (2 Tail)**** | | | | | |
| Distance | **0.00** | 0.61 | **0.00** | **0.00** | 0.13 |
| Angle | 0.92 | **0.00** | 0.17 | 0.18 | **0.03** |
| Power | 0.43 | **0.00** | 0.07 | **0.01** | 0.05 |
| Pressure | **0.00** | 0.17 | **0.00** | 0.34 | 0.94 |
| Predicted Max. Adhesion (psi) | 1434 | 2484 | 1177 | 1566 | 2544 |
| $r^2$ | 0.86** | 0.78 | 0.95 | 0.76 | 0.34 |

* If the coefficient p is less than 0.05, then it is considered statistically significant. These are shown in bold type.

** The factor $r^2$ is the square of the regression coefficient R, which is a measure of the proportion of the data accounted for by the regression equation.

The expected adhesion pull-off values vary widely from material to material. In order of magnitude, the ranking of adhesion is material 5 (Al:$AlO_2$), material 2 (Al), material 4 (Zn:Al pseudo), material 1 (Zn:Al), and material 3 (Zn). The magnitudes of the coefficients associated with each application factor give one indication of the degree to which that factor dictates coating adhesion. The direction of this influence is given by the sign of the coefficient. Positive values of a coefficient will increase adhesion as they are increased. The likelihood that the adhesion increase is linear (all other parameters being held constant) is expressed by the p coefficient.

Distance plays the strongest role in determining adhesion based on the results in Table 8. Uniformly, a shorter distance from gun to surface will result in higher adhesion pull-off readings. This is particularly marked for all except material 2, which is also the only sample set without a significant p coefficient in the 2-tail t-test.

The remainder of the results are more mixed, which may be an influence of the chemistry and metallurgy of the wires used for spraying the metallized coating. Contrast the coefficients of influence of power, pressure, and angle for samples that are pure zinc or zinc alloys (materials 1 and 3) with those for which free aluminum is available (all others). Materials 2 and 5 have the highest level of aluminum (100% and 90% respectively), and both show increased adhesion with increased power to the gun based on their coefficients of 300.7 and 107.5, respectively. The p coefficients for power to the gun are also highly significant for these two materials. The third free aluminum containing wire feed stock (material 4, the pseudo alloy) also shows a significant p coefficient for power to the gun. Material 4 has a lower order of magnitude for the influence coefficient at 30.2.

A similar trend is observed in the influence of pressure at the gun on adhesion, though this is far less dramatic than power to the gun. This trend is best seen by looking at the p coefficients for the pure zinc-containing alloys (materials 1 and 3). Both true zinc alloy specimens show improved adhesion with lower pressure at the gun, and for both this trend is significant as indicated by the p coefficient. Materials containing free aluminum tend to show weakly positive (materials 4 and 5) or negative association between adhesion and pressure. In all cases, the influence of pressure at the gun is insignificant if metallic aluminum is used.

Angle to the surface provides another striking contrast between the zinc alloy and aluminum samples. It also provides a conundrum. The influence factors for materials 1 and 3 are as expected, positive, indicating that higher angles (close to perpendicular) will result in improved adhesion. Adhesion is predicted to

decrease as the angle of application reaches its default value of 90 degrees, based on the influence coefficients for materials 2, 4, and 5. This result simply does not make sense. It is suspected (but cannot be proven at this time) that this anomalous result is caused by the extreme response shown by materials 2, 5, and to a lesser extent 4, to increased power at the gun. Inspection of the original design matrix in Table 5 shows that, for a power of 450 amps at the gun, all angles were used, as expected. The suspected confounding is a second-order effect caused by combination of low angle with high power at high pressure and shorter distances.

### Analysis of Means for Adhesion

Another view of the role each application factor plays in determining adhesion is given by the ANOM plots. These are shown in full in Appendix B. Figure 6 is a typical ANOM plot (for material 1 adhesion). A summary of the evaluation of these plots for adhesion is given in Table 9. The slope of the lines provides visual confirmation that distance to the surface is indeed very influential on adhesion for material 1. Furthermore, the highest values for adhesion are readily picked from the chart (i.e., distance of 6 in., angle of 67.5 degrees, power to the gun of 450 amps, and pressure at the gun of 90 psi will probably provide highest adhesion). Note that the predicted values from modeling may differ, as this takes into account second-order interactions not readable in an ANOM plot.

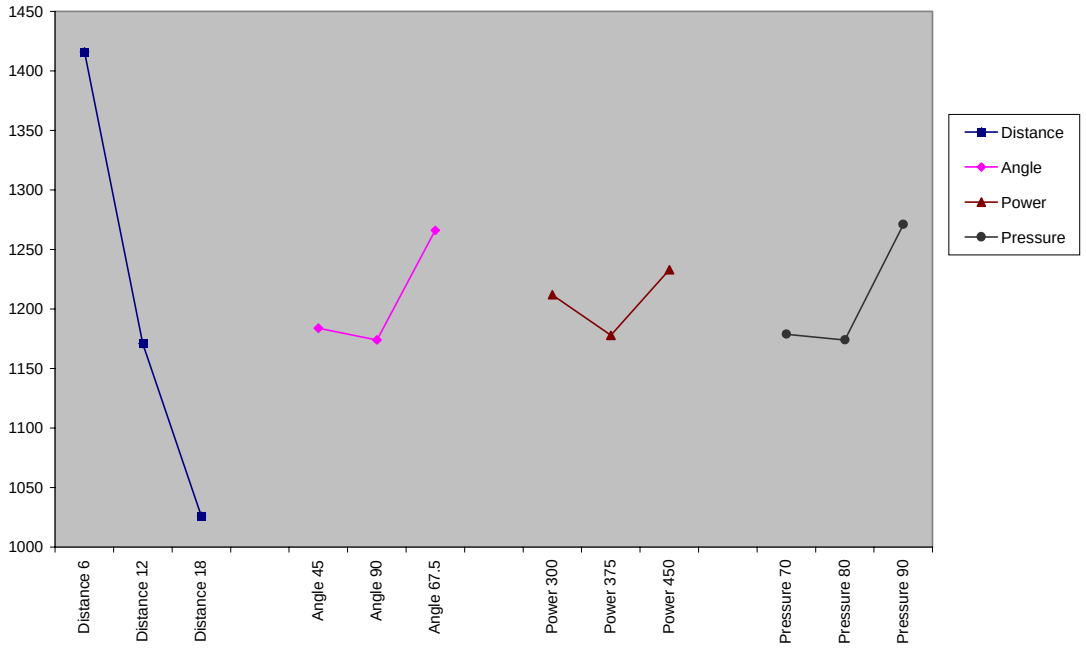


**Figure 6. Typical analysis of means plot — material 1 (Zn:Al 85:15) adhesion.**

The ANOM summary in Table 9 also provides the range of values seen in the plots and their approximate proportion relative to the mean for the pooled adhesion results. The mean pull-off for material 1 is approximatey 1,200 psi, while the mean pull-off for material 5 is approximately 2,100 psi. The range for material 1 is nearly 400 psi, approximately one-third of the pooled mean pull-off strength. The range for material 5 is little more than 200 psi, approximately one-tenth its pooled mean pull-off strength. The standard deviation of the 12 center-point samples and their coefficients of variation are also presented for each material in Table 9.

The information gleaned from the ANOM exercise helps to predict which factors should be emphasized in a model equation based on the coefficients from the Y Model.

#### Optimum Operational Settings to Maximize Adhesion

Table 10 gives the predicted operational settings to maximize adhesion for the nine samples of each material in the Taguchi L9 matrices. Suggested settings for application parameters are contrasted with the predictions made based on the ANOM. With the exception of the suggested values for angle of the gun for materials 3 and 4, and pressure at the gun for material 1, all settings are consistent with the predicted ranges from the ANOM plots. Once again, it is vital that these results be interpreted with great care. It is highly doubtful that an angle of application of 45 degrees is truly ideal for any coating material. Confounding of effects is once again suspected with low angle of incidence samples displaying the benefit of other less troublesome changes to operation settings for application.

As with any statistical modeling exercise, it is essential that steps be taken to confirm a tentative (not to say controversial) hypothesis. The raw data for adhesion pull-off strength (Tables B1 through B6) show high values for adhesion pull-off strength for samples at close distances and also unusual gun to sample angles. Thus, the output from the model reflects the input to the model.

**Table 9. Adhesion pull-off testing analysis of means summary.**

| Material | Primary Effects by Inspection | Optimum Setting by Inspection | Rough Range and Mean of Plot (rounded) | Standard Deviation | Coefficient of Variation |
|---|---|---|---|---|---|
| (1) Zn:Al 85:15 | Distance | D 6, A 67.5, Po 375-450, Pr 90 | Range 400<br>Mean 1200 | 67 | 0.059 |
| (2) Aluminum | Angle, Power | D 6, A 45, Po 450, Pr 70 | Range 700<br>Mean 1900 | 141 | 0.080 |
| (3) Zinc | Distance | D 6, A 90 - 67.5, Po 375-450, Pr 80-90 | Range 400<br>Mean 900 | 48 | 0.060 |
| (4) Zn:Al (85:15) Pseudo | Distance | D 6, A 90, Po 450, Pr 70-90 | Range 300<br>Mean 1400 | 37 | 0.027 |
| (5) Al:$AlO_2$ (90:10) | Distance, Angle, Power, Pressure | D 6, A 45, Po 450, Pr 90 | Range 200<br>Mean 2100 | 99 | 0.053 |

* The values for standard deviation and coefficient of variation are taken from descriptive statistics for the 12 center-point samples. They provide a measure of the "dispersion" in the experimental results.

**Table 10. Comparison of ANOM and multiple linear regression model optimum settings for adhesion.**

| | Material 1 Zn:Al (85:15) | Material 2 Aluminum | Material 3 Zinc | Material 4 Zn:Al (85:15) Pseudo | Material 5 Al:$AlO_2$ (90:10) |
|---|---|---|---|---|---|
| ***Optimized Settings From Multiple Linear Regression*** | | | | | |
| Distance | 6 | 6 | 6 | 6 | 6 |
| Angle | 68 | 45 | 45 | 71 | 45 |
| Power | 300 | 450 | 387 | 450 | 450 |
| Pressure | 70 | 70 | 85 | 70 | 80 |
| Predicted Maximum Adhesion (psi) | 1434 | 2484 | 1177 | 1566 | 2544 |
| ***ANOM Suggested Settings*** | | | | | |
| Distance | 6 | 6 | 6 | 6 | 6 |
| Angle | 67.5 | 45 | 67.5 | 90 | 45 |
| Power | 375-450 | 450 | 375-450 | 450 | 450 |
| Pressure | 90 | 70 | 80-90 | 70-90 | 80 |

### *Influence of Application Parameters on Erosion Weight Loss*

Operational settings to minimize erosion weight loss are given in Table 11. The data are presented based upon a multiple linear regression analysis of the L9 matrix.

**Table 11. Predicted erosion, degree of factor influence, and probability coefficients from Taguchi modeling of erosion weight loss results (L9 matrix only).**

| | Material 1 Zn:Al (85:15) | Material 2 Aluminum | Material 3 Zinc | Material 4 Zn:Al (85:15) Pseudo | Material 5 Al:$AlO_2$ (90:10) |
|---|---|---|---|---|---|
| ***Coefficients of influence on the regression equation*** | | | | | |
| Distance | 0.0028 | 0.0031 | 0.0303 | 0.0122 | 0.0057 |
| Angle | -0.0257 | -0.0024 | -0.0225 | -0.0063 | 0.0027 |
| Power | -0.0036 | -0.0046 | 0.0026 | -0.0033 | -0.0012 |
| Pressure | 0.0216 | -0.0007 | -0.0140 | -0.0022 | -0.0047 |
| ***Probability Coefficients P (2 Tail)**** | | | | | |
| Distance | 0.8835 | **0.0017** | **0.0000** | **0.0035** | **0.0000** |
| Angle | 0.1966 | **0.0113** | **0.0000** | 0.1021 | **0.0000** |
| Power | 0.8523 | **0.0000** | 0.4701 | 0.3700 | **0.0059** |
| Pressure | 0.2745 | 0.4278 | **0.0010** | 0.5482 | **0.0000** |
| Predicted Erosion Weight Loss (g) | 0.05 | 0.039 | 0.11 | 0.065 | 0.038 |
| $r^2$ | 0.32** | 0.78 | 0.89 | 0.49 | 0.97 |

* If the coefficient p is less than 0.05, then it is considered statistically significant. These are shown in **bold** type.

** The factor $r^2$ is the square of the regression coefficient R. This is a measure of the proportion of the data accounted for by the regression equation.

The material with the highest level of apparent resistance to erosion weight loss is material 5 (Al:$AlO_2$). In fact, this resistance is touted as a benefit of this ceramic metallic material. Overall, the degree of additional protection afforded by this material is modest compared to the standard 85:15 Zn:Al alloy (material 1). Pure aluminum works nearly as well in resisting erosion weight loss. The best to worst ranking of the materials for erosion resistance is: material 5 (Al:$AlO_2$) = material 2 (Al); material 1 (Zn:Al); material 4 (Zn:Al pseudo); then material 3 (Zn). The erosion loss correlates roughly with the amount of zinc (the higher the level of zinc, the higher the weight losses measured).

The order of magnitude of the coefficients of influence for each parameter is much closer to that of typical erosion readings, which is in marked contrast to adhesion pull-off testing. This indicates a higher variability in the measurements (see the discussion of ANOM below).

Based on the 2-tail p coefficients, aluminum bearing metallized samples (materials 2 and 5) show sensitivity to angle of application and to power applied to the gun. Unlike the case with adhesion, however, the direction of the influence of angle is identical with that of power. This result suggests that erosion weight losses will diminish more sharply for these materials as the angle of application reaches 90 degrees. (The coefficient of influence is identical for all materials,

though sensitivity as suggested by the p coefficients is much lower outside of materials 2 and 5.) Increased power to the gun also improved adhesion for these samples. It seems intuitively correct that higher adhesion would correspond with reduced cavitation/erosion weight losses.

The coefficient for distance from the surface is positive for all materials. This means that higher erosion weight losses occur the further away from the surface the gun is during application. This factor is statistically significant for all materials except material 1 (Zn:Al 85:15 alloy). Thus, the expected optimum settings will likewise favor closer approaches to the surface, as was the case in the adhesion modeling. Pressure at the gun is only of significant influence for materials 3 and 5. Reduced pressure at the gun is likely to reduce weight losses in cavitation/erosion for these materials.

Erosion losses for material 1 (Zn:Al alloy), which is probably one of the most widely specified thermal spray compositions, seem largely insensitive to changes in any of the application parameters.

#### Analysis of Means for Erosion Weight Loss

With the exception of material 5 (Al:$ALO_2$ 90:10 alloy), the expected angle for application is more reasonable than was the case for adhesion. The plot of ANOM for each material is summarized in the bottom portion of Table 12. The actual plots themselves are in Appendix C. The last rows display the mean and range for the nine samples undergoing the analysis. Following these are the standard deviation and coefficient of variation for the 12 center-point samples for each material. Table 12 underscores how large the range of results is compared to the mean erosion weight loss exhibited by the pooled samples for each material. The ratio between mean and range is near unity for material 1, which is consistent with the high coefficient of variation for the center-point samples. For all other materials, it is a significant fraction of the mean erosion weight loss value. A separate table describing which of the application factors is most significant is not supplied for erosion weight loss. Significant application factors are assigned based on inspection of the slope of the ANOM plot lines. Such factors are indicated in bold print within the lower portion of Table 12. Note that material 1, for which no application parameter showed strong influence based on the p coefficients in Table 12, shows strong dependence on the specific settings noted. Most of the suggested settings for material 1 are close to, or encompass, the center-point settings for application.

**Table 12. Comparison of ANOM and multiple linear regression model optimum settings for erosion resistance.**

| | Material 1 Zn:Al (85:15) | Material 2 Aluminum | Material 3 Zinc | Material 4 Zn:Al (85:15) Pseudo | Material 5 Al:$AlO_2$ (90:10) |
|---|---|---|---|---|---|
| ***Optimized Settings From Multiple Linear Regression*** | | | | | |
| Distance | **6** | **6** | **6** | **6** | **6** |
| Angle | **81** | **45** | **82** | **45** | **45** |
| Power | **300** | **450** | **300** | **421** | **390** |
| Pressure | **76** | **70** | **70** | **70** | **84** |
| Predicted Minimum Erosion (g) | **0.0** | **0.03** | **0.06** | **0.06** | **0.2** |
| ***ANOM Suggested Settings*** | | | | | |
| Distance | **6, 18** | **6** | **6** | **6** | **6** |
| Angle | **67.5 - 90** | **67.5** | **67.5** | **67.5** | 45 |
| Power | **300, 450** | **450** | 300-375 | 375-450 | 375-450 |
| Pressure | **80** | **90** | **90** | 90 | **80-90** |
| Mean (Rounded) | 0.05 | 0.04 | 0.10 | 0.07 | 0.04 |
| Range (Rounded) | 0.05 | 0.01 | 0.06 | 0.03(5)* | 0.02 |
| Standard Deviation | 0.04 | 0.00(2) | 0.01 | 0.01 | 0.00(2) |
| Coefficient of Variation | 0.78 | 0.05 | 0.11 | 0.12 | 0.04 |

* Data points that are less than unity are rounded up to the second digit unless the third digit is exactly 5, or the third digit is the first significant digit. For these exceptions the third digit is shown in parentheses.

### Optimum Operational Settings To Maximize Cavitation Erosion Resistance

The recommended settings from the Y model to optimize erosion resistance are given in the top portion of Table 12. For distance to the surface, the suggested settings to minimize erosion weight loss are in keeping with the general trend found in the ANOM analysis. For angle of application, the Y model is not consistent with the ANOM. Again a note of caution, this modeling should not be taken to suggest that an unusual angle of application is ideal. All other results are largely consistent between the ANOM and multiple linear regression exercises.

### *Influence of Application Parameters on Porosity and Oxide Content*

Table 13 summarizes the main coefficients for application factors through modeling of the image analysis (porosity and oxide content) using a multiple linear regression analysis of the L9 matrix.

The poorest film results in terms of porosity and oxide content are those for material 4 — Zn:Al pseudo alloy (0.22 or over one-fifth of the layer has pores or oxide inclusions). Material 4 exhibited the largest amount of interlayer laminar

voids, perhaps as a consequence of its method of mixing the two metals at the gun. The results for material 5 ($Al/AlO_2$) are close to those for material 4. Given that the alloy already contains 10% $AlO_2$ and that the image quality for material 5 samples was exceptionally poor, this result is better than expected. Porosity and oxide content can be ranked in the following order: material 1 is > material 3, is > material 2, is > material 4, is essentially equal to material 5.

The values in Table 13 suggest that a closer approach will reduce porosity and oxide formation. All vectors for the coefficients of influence for distance to the surface are positive, so increasing distance increases porosity. This conclusion is intuitively reasonable. The greater the distance from the gun to the sample surface, the greater the risk of oxidation at the extremes of the plasma shroud. The longer the path that the thermal spray particles travel, the greater the risk of agglomeration, resulting in voids.

The coefficients for angles of application for all materials are negative, indicating that an increase in angle (towards 90 degrees) will reduce porosity and oxide content. This conclusion also seems reasonable. The influence of power at the gun is only significant for material 1, for which lower powers will reduce porosity. Pressure has a negative coefficient, which suggests that lower pressures at the gun will improve film quality.

**Table 13. Predicted porosity/oxide, degree of factor influence and probability coefficients from Taguchi modeling of image analysis results (L9 matrix only).**

| | Material 1 Zn:Al (85:15) | Material 2 Aluminum | Material 3 Zinc | Material 4 Zn:Al (85:15) Pseudo | Material 5 Al:$AlO_2$ (90:10) |
|---|---|---|---|---|---|
| ***Coefficients of influence on the regression equation*** | | | | | |
| Distance | 0.0261 | 0.0022 | 0.0217 | 0.0083 | 0.0100 |
| Angle | -0.0267 | -0.0078 | -0.0294 | -0.0072 | -0.0283 |
| Power | 0.0144 | 0.0039 | 0.0028 | -0.0061 | -0.0044 |
| Pressure | -0.0028 | -0.0078 | -0.0039 | -0.0044 | -0.0350 |
| ***Probability Coefficients P (2 Tail)**** | | | | | |
| Distance | **0.0004** | 0.6231 | **0.0035** | 0.1673 | 0.5967 |
| Angle | **0.0004** | 0.0971 | **0.0002** | 0.2284 | 0.1443 |
| Power | **0.0286** | 0.3931 | 0.6717 | 0.3053 | 0.8135 |
| Pressure | 0.6526 | 0.0971 | 0.5539 | 0.4528 | 0.0756 |
| Predicted Minimum Porosity (Proportion) | 0.0800 | 0.1500 | 0.1100 | 0.2200 | 0.2000 |
| $r^2$ | 0.73** | 0.42 | 0.66 | 0.38 | 0.43 |

* If the coefficient p is < 0.05, then it is considered statistically significant. These are shown in bold type.

** The factor $r^2$ is the square of the regression coefficient R; this is a measure of the proportion of the data accounted for by the regression equation.

Zinc alloy samples (materials 1 and 3) both exhibit strong p coefficients for influence of distance to surface and angle of gun. None of the aluminum materials show statistically significant p coefficients from the 2-tail t-test. None of the p factors for pressure at the gun is statistically significant. Those for pure Al and Al:$AlO_2$ alloy do show reasonably small values.

The Zn:Al pseudo alloy does not exhibit statistically significant sensitivity to any application factor.

### Analysis of Means for Porosity and Oxide Content

The suggested settings to minimize porosity and oxide content from the ANOM are summarized in Table 14. Those factors with strong influence (identified by a steep slope) are shown in bold font. Above these settings are those suggested by the optimization of the model derived from multiple linear regression on the Taguchi L9 arrayed results.

**Table 14. Predicted optimum settings for minimizing porosity and oxide content — ANOM and Taguchi l9 array only.**

| | Material 1 Zn:Al (85:15) | Material 2 Aluminum | Material 3 Zinc | Material 4 Zn:Al (85:15) Pseudo | Material 5 Al:$AlO_2$ (90:10) |
|---|---|---|---|---|---|
| ***Optimized Settings From Multiple Linear Regression*** | | | | | |
| Distance | 6 | 6 | 6 | 11 | 6 |
| Angle | 86 | 45 | 90 | 74 | 45 |
| Power | 300 | 351 | 313 | 450 | 382 |
| Pressure | 70 | 70 | 70 | 82 | 83 |
| Optimized Minimum Porosity (Proportion) | 0.03 | 0.14 | 0.05 | 0.16 | 0.18 |
| ***ANOM Suggested Settings*** | | | | | |
| Distance | **6** | 6-18 | **6** | **12** | 6-18 |
| Angle | **67.5-90** | **67.5** | **67.5** | **90** | 67.5 |
| Power | **300** | 375 | 300-450 | 375-450 | 375-450 |
| Pressure | 90 | 70-90 | 70-90 | 80 | **80** |
| Mean (Rounded) | 0.09 | 0.14 | 0.11 | 0.19 | 0.25 |
| Range (Rounded) | 0.07 | 0.025 | 0.07 | 0.03 | 0.12 |
| Standard Deviation | 0.015 | 0.025 | 0.016 | 0.025 | 0.023 |
| Coefficient of Variation | 0.178 | 0.240 | 0.170 | 0.162 | 0.098 |

Of the five materials, material 1 has the highest ratio between the range and mean. Material 1 also has the lowest overall porosity and oxide content of any material tested here.

#### Optimum Levels for Minimizing Porosity and Oxide Content

For material 1, the only application setting not in agreement between the ANOM and multiple regression analysis is the less sensitive factor of atomizing pressure at the gun. Angle of the gun once again appears not to have been well defined as an optimum by either the ANOM or multiple regression. For material 2, the suggested value for the angle from multiple linear regression is lower than suggested by ANOM, indicating that either confounding of effects is occurring, or a local minimum has been found in the surface model. For material 3, a higher level of angle to the surface is predicted by multiple linear regression than by ANOM. For material 4, the multiple linear regression model predicts a lower angle than the ANOM. Note that angle to the surface was only a significant factor for materials 1 and 3 in the regression modeling.

### *Taguchi Modeling to Minimize Variation (S Model)*

Another important feature of the Taguchi analysis is the S model. The Taguchi S model helps define the influence that an application parameter has on eliminating variation in film properties. The data output is the expected standard deviation under a defined set of application conditions. The sensitivity of the standard deviation to changes in the value of an application parameter is also assessed.

The expectation is that limiting variation will result in more uniform performance. Computation of predicted standard deviations (and of settings to minimize the standard deviation) are made using equations identical in format to those for the Y model, Equations 1 through 5, pages 32 to 35.

A condensed form of the output from the S models for each material and performance characteristic is given in Tables 15 through 17. Application parameters are deemed influential if the p coefficient is less than or equal to 0.05 (statistically significant). The data provided in the following section are based on two distinct types of S models. The first S model is the pure L9 matrix. The coefficient for each application parameter and suggested settings to minimize standard deviations are taken from this S model. The second S model uses the results from all 21 samples of each material. This matrix contains 12 repeat samples at the center-point application settings. The 2-tail t-test is possible.

From the t-test, an estimate of the statistical significance of each application parameter's influence on standard deviation (variation in performance) is inferred.

**Table 15. Summary of S model output for adhesion pull-off strength.**

| Adhesion | Coefficient | P(2-Tail) * | Suggested Settings |
|---|---|---|---|
| Constant | 63.395 | 0.030 | |
| Distance | -21.083 | 0.095 | 16 |
| Angle | 8.013 | 0.364 | 64 |
| Power | -17.489 | 0.159 | 300 |
| Pressure | -16.293 | 0.187 | 70 |
| **Predicted S Value** | | **53** | **Material 1** |
| Constant | 85.821 | 0.052 | |
| Distance | 5.436 | 0.884 | 12 |
| Angle | -18.897 | 0.615 | 72 |
| Power | 45.351 | 0.237 | 345 |
| Pressure | -49.579 | 0.199 | 70 |
| **Predicted S Value** | | **32** | **Material 2** |
| Constant | 40.965 | 0.000 | |
| Distance | -15.279 | **0.000** | 16 |
| Angle | 7.268 | 0.238 | 45 |
| Power | 0.728 | 0.255 | 300 |
| Pressure | 1.791 | **0.000** | 70 |
| **Predicted S Value** | | **7** | **Material 3** |
| Constant | 51.305 | 0.000 | |
| Distance | 0.746 | 0.876 | 12 |
| Angle | 1.997 | 0.154 | 45 |
| Power | 6.111 | 0.216 | 300 |
| Pressure | 3.101 | 0.520 | 80 |
| **Predicted S Value** | | **8** | **Material 4** |
| Constant | -0.932 | 0.255 | |
| Distance | 94.637 | **0.009** | 10 |
| Angle | 72.751 | **0.003** | 62 |
| Power | -63.005 | 0.061 | 450 |
| Pressure | 96.998 | **0.008** | 70 |
| **Predicted S Value** | | **-186** | **Material 5** |

* - The p coefficients use data from all 21 samples. All other data is based on analysis of the L9 matrix alone.

**Table 16. Summary of S model output for erosion weight loss.**

| Erosion | Coefficient | P(2Tail) * | Suggested Settings |
|---|---|---|---|
| Constant | 0.087 | 0.380 | |
| Distance | 0.000 | 0.995 | 6 |
| Angle | -0.042 | 0.798 | 79 |
| Power | 0.001 | 0.957 | 300 |
| Pressure | 0.040 | 0.170 | 74 |
| **Predicted S Value** | | **-0.091** | **Material 1** |
| Constant | 0.001 | 0.198 | |
| Distance | 0.000 | 0.951 | 12 |
| Angle | -0.002 | 0.759 | 78 |
| Power | 0.000 | 0.731 | 340 |
| Pressure | -0.001 | 0.592 | 70 |
| **Predicted S Value** | | **0.000** | **Material 2** |
| Constant | 0.022 | 0.000 | |
| Distance | -0.002 | **0.000** | 6 |
| Angle | 0.004 | **0.000** | 45 |
| Power | -0.003 | **0.000** | 300 |
| Pressure | -0.001 | **0.000** | 70 |
| **Predicted S Value** | | **0.012** | **Material 3** |
| Constant | 0.012 | 0.001 | |
| Distance | 0.004 | **0.039** | 6 |
| Angle | -0.005 | 0.218 | 90 |
| Power | 0.001 | 0.692 | 302 |
| Pressure | 0.003 | 0.154 | 71 |
| **Predicted S Value** | | **0.002** | **Material 4** |
| Constant | 0.002 | 0.622 | |
| Distance | 0.000 | 0.996 | 6 |
| Angle | 0.001 | 0.906 | 45 |
| Power | 0.000 | 0.994 | 450 |
| Pressure | 0.000 | 0.991 | 70 |
| **Predicted S Value** | | **0.000** | **Material 5** |

* - The p coefficients use data from all 21 samples. All other data are based on analysis of the L9 matrix alone.

**Table 17. Summary of S model output for porosity and oxide content.**

| Porosity and Oxide | Coefficient | P(2 Tail) * | Suggested Settings |
|---|---|---|---|
| Constant | 0.012 | 0.079 | |
| Distance | 0.009 | **0.045** | 10 |
| Angle | -0.002 | 0.188 | 69 |
| Power | 0.009 | **0.037** | 300 |
| Pressure | -0.001 | 0.811 | 70 |
| **Predicted S Value** | | **-0.011** | **Material 1** |
| Constant | 0.020 | 0.007 | |
| Distance | 0.001 | 0.864 | 12 |
| Angle | -0.001 | 0.804 | 45 |
| Power | 0.003 | 0.633 | 300 |
| Pressure | 0.003 | 0.608 | 70 |
| **Predicted S Value** | | **0.007** | **Material 2** |
| Constant | 0.035 | 0.000 | |
| Distance | 0.012 | **0.003** | 6 |
| Angle | 0.000 | 0.581 | 66 |
| Power | 0.002 | 0.457 | 300 |
| Pressure | -0.002 | 0.618 | 70 |
| **Predicted S Value** | | **0.004** | **Material 3** |
| Constant | 0.010 | 0.041 | |
| Distance | 0.007 | 0.193 | 6 |
| Angle | 0.003 | 0.181 | 65 |
| Power | 0.003 | 0.513 | 361 |
| Pressure | 0.005 | 0.298 | 70 |
| **Predicted S Value** | | **-0.002** | **Material 4** |
| Constant | 0.079 | 0.000 | |
| Distance | 0.028 | **0.012** | 10 |
| Angle | -0.002 | **0.019** | 45 |
| Power | 0.009 | 0.351 | 300 |
| Pressure | -0.026 | **0.019** | 84 |
| **Predicted S Value** | | **-0.035** | **Material 5** |

* The p coefficients use data from all 21 samples. All other data are based on analysis of the L9 matrix alone.

Because of the orthogonal nature of the L9 matrix, $r^2$ is set at unity, which is not a reliable indicator of the fitness of the S model to predict operating settings that result in minimal standard deviation. The quality of fit of the S models described by the coefficients in Tables 15 to 17 is indirectly inferred by cross-reference to the $r^2$ values for the parent Y model and direct reference to the p coefficients associated with the second S model. If the Y model has a low value of $r^2$ and the 2-tail t-test indicates a high level of significance, then one can reasonably assume that the predicted minimum standard deviation is reasonable. On occasion, the S model will resolve to a local minimum that shows a negative value for the standard deviation. Occurrences of such negative values are also

cause to question the fitness of the S model for that material. The following section examines each material tested for these significant factors.

### Discussion of Significant Application Parameters, Material 1 – Zn:Al (85:15)

- *Adhesion* — Variation in adhesion pull-off strength has no influential parameters, though distance to surface has the lowest p coefficient. Suggested settings to reduce adhesion variation are identical with those to maximize adhesion pull-off strength for all factors except distance. As none of the p coefficients in the S model are statistically significant, greater weight is given to the suggested settings from the Y model that maximize adhesion.
- *Erosion weight loss* — Variation in erosion weight loss is not significantly influenced by any application parameter. This suggests consideration of settings that maximize resistance to erosion weight loss and de-emphasizes settings that reduce variation.
- *Porosity and oxide content* — Both distance to the sample and power applied to the gun significantly influence variation in porosity and oxide content. To reduce variation, a distance of 10 in. is suggested. To maximize film quality, a distance of 6 in. is suggested. The suggested value for power to the gun is identical with that in the Y model. The $r^2$ value in the Y model is 0.74. It is inferred that S model settings for distance and power should be included in the overall settings for application of this material.
- Overall settings to maximize all performance attributes for material 1, while reducing variation are:
  — Distance to the surface - 6 to 10 in.
  — Angle of gun - 90 degrees
  — Power to the gun - 300 amps
  — Pressure at the gun - 90 psi

### Discussion of Significant Application Parameters for Material 2 – Aluminum

None of the application parameters had a statistically significant influence on minimizing variation in adhesion, erosion weight loss, or porosity and oxide content. This suggests that one can adopt the optimum settings to enhance these performance properties, without risking excessive variation in quality.

Suggested settings for material 2, which can maximize performance properties without suffering excessive variation, are:

- Distance to the surface - 6 to 11 in.
- Angle of gun - 90 degrees

- Power to the gun - 450 amps
- Pressure at the gun - 90 psi

**Discussion of Significant Application Parameters for Material 3 – Zinc**

- *Adhesion* — Both distance and pressure are influential parameters affecting variation in adhesion. The $r^2$ value from the Y model is 0.95, from which it is inferred that the results of both the Y and S models must be taken into account. t is informative to look at the scale of the coefficients for distance in both models. That coefficient is -170 for the Y model, while the S model is an order of magnitude lower at -15.3. Both coefficients are negative, which suggests that increasing distance will reduce adhesion strength, while it has a marginal impact on reduced variation in adhesion. It is suggested that preference be given to settings that maximize achievable adhesion in this instance.
- *Erosion weight loss* — All application variables are influential on variation in erosion weight loss. With the exception of the suggested values for angle at the gun (45 degrees vs. 82 degrees in the Y model), all settings agree with those in the Y model.
- *Porosity and oxide content* — Only distance to the sample is influential on variation in porosity and oxide content. The suggested distance to the sample is 6 in., which is identical with the distance suggested to minimize porosity and oxide content.
- Suggested settings to maximize performance while minimizing variation are listed below:
  - Distance to the surface - 6 in.
  - Angle of gun - 90 degrees (unless a re-evaluation of the suggested settings confirms the given lower values)
  - Power to the gun - 400 amps
  - Pressure at the gun - 90 psi

**Discussion of Significant Application Parameters for Material 4 – Zn:Al (85:15) Pseudo Alloy**

Variations in adhesion pull-off strength and porosity and oxide content have no influential parameters. This suggests that one can adopt the optimum settings to maximize adhesion, without risking excessive variation in quality.

- *Erosion weight loss* — Variation in erosion weight loss has only one parameter of significant influence, distance to surface. The suggested settings for distance are identical in both the Y and S models at 6 in.

- Suggested settings to maximize performance and minimize variation are:
  — Distance to the surface - 6 in.
  — Angle of gun - 90 degrees
  — Power to the gun - 350 to 400 amps
  — Pressure at the gun - 80 to 90 psi

**Discussion of Significant Application Parameters for Material 5 – Al/ $AlO_2$ (90:10) Alloy**

- *Adhesion* — All parameters except power to the gun have an influential effect on variation in adhesion pull-off strength. The settings are close between the S and Y models for power to the gun (450 amps) and pressure at the gun (Y model, 80 psi, S model 70 psi). The setting for distance is larger in the S model at 10 in. The S model resolves to a local minimum showing a negative value, which, along with a low value (0.34) for $r^2$ in the Y model, indicates that neither model correctly profiles the expected adhesion performance of this material.
- *Erosion weight loss* — None of the application parameters appear to be influential on variation in erosion weight loss. Suggested settings from the Y model are given precedence.
- *Porosity and oxide content* — The S model resolves to a local minimum with a negative value for predicted standard deviation. This, along with a low value (0.43) for $r^2$ in the Y model, draws into question the fit between the models and expected porosity for material 5. Only power to the gun is not influential on variation in porosity and oxide content. Angle of the gun was also influential on minimizing the amount of porosity and oxide content of samples. The value for angle of the gun to minimize variation is nearly coincident with that for minimizing the amount of porosity and oxide content (90 degrees).
- Suggested settings to maximize performance without risking excessive variation in performance are:
  — Distance to the surface - 6 to 10 in.
  — Angle of gun - 90 degrees
  — Power to the gun - 390 amps
  — Pressure at the gun - 80 to 90 psi.

## Analysis of Precision From Outer Arrays

This section presents the summary statistics for the outer array of 12 samples. The primary issue is whether the standard deviation of this population of samples is larger than the estimated standard error for each of the Taguchi L9 (TL9) arrays. This information is shown in Table 18. The standard error of means of

TL9 array is typically three times that of outer array. Standard deviation diverges by similar order of magnitude. This hints that the "within-lab error" is low compared to variation due to altering angle, distance to the surface, and power or pressure at the gun.

## Effect of Abrasive Type and Surface Profile Depth on Adhesion Performance

The adhesion performance of a subset of samples was examined (see Table 19) using multiple linear regression to determine the optimum conditions for surface preparation. The default surface preparation method using $AlO_2$ (to create a nominal 3-mils profile) was one factor in the design. The other factor called for the use of a steel shot abrasive. The effect of profile was examined at two levels, 1 mil and 3 mils, for both the steel shot and $AlO_2$. The respective shape of the two abrasives (and the resulting profile shape — round versus angular) is also believed to play a role in optimizing adhesion, though this was not thoroughly quantified.

**Table 18. Standard deviations for outer arrays compared to L9 array and all samples.**

| | Standard Deviations | | | Standard Errors | |
|---|---|---|---|---|---|
| Performance Measures | All Samples | L9 Samples | Outer Array | Outer Array | L9 Array |
| **Adhesion** | | | | | |
| Material 1 | 130.42 | 180.17 | 66.64 | 19.23 | 60.00 |
| Material 2 | 230.08 | 291.92 | 141.00 | 40.70 | 97.31 |
| Material 3 | 123.14 | 159.81 | 48.34 | 13.95 | 53.27 |
| Material 4 | 74.38 | 107.89 | 36.63 | 10.57 | 35.96 |
| Material 5 | 179.02 | 194.41 | 98.72 | 28.50 | 64.80 |
| **Erosion** | | | | | |
| Material 1 | 0.03 | 0.04 | 0.02 | 0.01 | 0.02 |
| Material 2 | 0.01 | 0.01 | 0.00 | 0.00 | 0.00 |
| Material 3 | 0.04 | 0.06 | 0.01 | 0.00 | 0.02 |
| Material 4 | 0.01 | 0.01 | 0.01 | 0.00 | 0.01 |
| Material 5 | 0.17 | 0.01 | 0.20 | 0.01 | 0.00 |
| **Porosity** | | | | | |
| Material 1 | 0.04 | 0.05 | 0.04 | 0.01 | 0.01 |
| Material 2 | 0.03 | 0.01 | 0.03 | 0.01 | 0.01 |
| Material 3 | 0.02 | 0.03 | 0.02 | 0.01 | 0.01 |
| Material 4 | 0.03 | 0.02 | 0.03 | 0.01 | 0.01 |
| Material 5 | 0.04 | 0.06 | 0.02 | 0.01 | 0.02 |

**Table 19. Average adhesion pull-off strength for each material, and contribution and significance of abrasive and profile depth to adhesion.**

| | | Material 1 | | Material 2 | | Material 3 | | Material 4 | | Material 5 | |
|---|---|---|---|---|---|---|---|---|---|---|---|
| Abrasive | Depth (mils) | Zn:Al 85:15 Alloy | | Aluminum | | Zinc | | Zn:Al 85:15 Pseudo | | Al:$AlO_2$ 90:10 Alloy | |
| | | Pull-Off Strength (psi) | | Pull-Off Strength (psi) | | Pull-Off Strength (psi) | | Pull-Off Strength (psi) | | Pull-Off Strength (psi) | |
| Aluminum Oxide | 1 | 1031 | | 1627 | | 789 | | 1170 | | 1618 | |
| Aluminum Oxide | 3 | 1210 | | 1819 | | 862 | | 1427 | | 1880 | |
| Steel Shot | 1 | 101 | | 1072 | | 107 | | 2005 | | 819 | |
| Steel Shot | 3 | 291 | | 1079 | | 103 | | 3209 | | 807 | |
| | | Coefficient | P 2 Tail | Coefficient | P 2 Tail | Coefficient | P 2 Tail | Coefficient | P 2 Tail | Coefficient | P 2 Tail |
| | Constant | 658.2 | | 1398.9 | | 465.4 | | 1952.7 | | 1281 | |
| | Abrasive | -462.3 | 0.0000 | -323.7 | 0.0000 | -360.2 | 0.0000 | 654.5 | 0.0004 | -468 | 0.0000 |
| | Depth | 92.3 | 0.0000 | 49.8 | 0.0318 | 17.3 | 0.0112 | 365.2 | 0.0251 | 62.5 | 0.0030 |
| | AB | 2.5 | 0.8066 | -46.2 | 0.0444 | -19.4 | 0.0055 | 236.6 | 0.1291 | -68.4 | 0.0015 |

The results of this surface preparation variation to the experimental design show a significant difference in the adhesion of each material. For all materials except the Zn:Al pseudo alloy, there was a substantial reduction in pull-off adhesion strength when using a metallic shot abrasive versus the $AlO_2$ oxide abrasive. For the four materials sharing this behavior, the ratio of adhesion for samples prepared with $AlO_2$ versus those prepared with metallic shot ranges from 10:1 to approximately 2:1. A smaller but statistically significant reduction in adhesion occurs when progressing from a higher profile depth to a lower profile depth. The improvement in adhesion afforded by a deeper profile is a characteristic of all five materials. This behavior coincides completely with conventional wisdom. A more complex angular profile, as provided by a mineral abrasive, is believed to improve adhesion. These results agree with this assumption. A deeper profile is often demanded for application of thermal spray materials, because they depend heavily on mechanical adhesion. Once again the results bear out this assumption.

The behavior shown by the Zn:Al pseudo alloy, which indicates higher adhesion for samples prepared by metallic shot, goes counter to the general trend of all other samples. For the Zn:Al pseudo alloy, the average adhesion pull-off strength with the use of the steel shot abrasive was approximately three times that of the same alloy applied to surface prepared using an $AlO_2$ abrasive. For materials 2, 3, and 5, adhesion shows a statistically significant dependence on the combined effects of abrasive and profile.

## Regression Analysis of Performance Parameters

### *Regression Analysis*

The influence of the operating parameters chosen for application on thermal spray coating physical characteristics and performance was assessed by conducting regression analyses. The average values for each of the three characteristics measured (adhesion pull-off tensile strength, cavitation/erosion weight loss, and porosity and oxide content) were independently regressed against each of the four operating parameters of distance, angle, power, and pressure. Average performance data for all 21 samples of each material were included in these regressions. This process pairs the dependent (observed measurements) against the independent (deliberately varied parameters) variables.

One purpose of this regression analysis was to confirm that the modeled influential parameters for each performance characteristic account for a significant fraction of the data. This result is assessed by looking at the values for $r^2$ contained in Table 20. Another goal was to compare the magnitude and vector of the correlation coefficients in Table 21 with the p coefficients in the Y and S models summarized in Tables 8 through 17. This exercise can help confirm the soundness of the models. Confirmation of the soundness of the model data occurs if instances of a low p coefficient (<0.05) coincide with a high correlation coefficient. If a high correlation coefficient does not coincide with low p coefficients from both the Y and S models, then the predictions from the model might be questionable.

### *Regression Analysis for Adhesion Data*

- *Adhesion and angle* — The values for $r^2$ suggest that the regression fit between these two variables accounts for less than half of the data (material 5 having the highest $r^2$ value). This validates the decision to ignore the unusual angle settings suggested by the Y and S models. None of the p coefficients in the corresponding Taguchi models is significant.
- *Adhesion and distance* — The values for $r^2$ suggest that adhesion is strongly linked to distance from the sample for materials 1, 3, and 4. All correlation coefficients for these materials are above 0.8; all $r^2$ values are above 0.9. This is the same relationship predicted from the Taguchi modeling results. The correlation coefficient vector is negative, supporting the suggestion that a low distance to the substrate will improve adhesion.
- *Adhesion and power* — Only for material 2 is there a strong correlation coefficient. This is consistent with the Taguchi model, which shows a very low (highly significant) p coefficient for this pair of variables.

- *Adhesion and pressure* — Neither the Y nor the S models suggest a strong relationship between adhesion and pressure. None of the regression coefficients for this variable pairing, for any material, is significant.

**Table 20. Regression coefficients for paired variables.***

| Coefficients | Material 1 | Material 2 | Material 3 | Material 4 | Material 5 |
|---|---|---|---|---|---|
| **Adhesion and Angle** | | | | | |
| Adjusted r^2 | 0.00 | 0.00 | 0.00 | 0.00 | 0.17 |
| Correlation Coefficient | 0.01 | -0.28 | 0.06 | 0.13 | -0.53 |
| **Adhesion and Distance** | | | | | |
| Adjusted r^2 | 0.86 | 0.00 | 0.83 | 0.82 | 0.01 |
| Correlation Coefficient | ***-0.94*** | -0.04 | ***-0.92*** | ***-0.92*** | -0.36 |
| **Adhesion and Power** | | | | | |
| Adjusted r^2 | 0.00 | 0.77 | 0.00 | 0.00 | 0.12 |
| Correlation Coefficient | 0.05 | ***0.89*** | 0.07 | 0.26 | 0.48 |
| **Adhesion and Pressure** | | | | | |
| Adjusted r^2 | 0.00 | 0.00 | 0.00 | 0.00 | 0.00 |
| Correlation Coefficient | 0.22 | -0.12 | 0.24 | 0.09 | 0.02 |
| **Erosion and Angle** | | | | | |
| Adjusted r^2 | 0.10 | 0.00 | 0.00 | 0.06 | 0.00 |
| Correlation Coefficient | -0.46 | -0.35 | 0.04 | -0.42 | 0.26 |
| **Erosion and Distance** | | | | | |
| Adjusted r^2 | 0.00 | 0.10 | 0.61 | 0.62 | 0.20 |
| Correlation Coefficient | 0.05 | 0.46 | ***0.81*** | ***0.81*** | 0.55 |
| **Erosion and Power** | | | | | |
| Adjusted r^2 | 0.00 | 0.40 | 0.00 | 0.00 | 0.00 |
| Correlation Coefficient | -0.06 | -0.69 | -0.33 | -0.22 | -0.12 |
| **Erosion and Pressure** | | | | | |
| Adjusted r^2 | 0.03 | 0.00 | 0.00 | 0.00 | 0.10 |
| Correlation Coefficient | 0.39 | -0.10 | 0.16 | -0.15 | -0.46 |
| **Porosity and Angle** | | | | | |
| Adjusted r^2 | 0.30 | 0.13 | 0.54 | 0.02 | 0.05 |
| Correlation Coefficient | -0.62 | -0.49 | **-0.77** | -0.37 | -0.41 |
| **Porosity and Distance** | | | | | |
| Adjusted r^2 | 0.28 | 0.00 | 0.23 | 0.07 | 0.00 |
| Correlation Coefficient | 0.61 | 0.14 | 0.57 | 0.43 | 0.15 |
| **Porosity and Power** | | | | | |
| Adjusted r^2 | 0.00 | 0.00 | 0.00 | 0.00 | 0.00 |
| Correlation Coefficient | 0.34 | 0.24 | 0.07 | -0.31 | -0.07 |
| **Porosity and Pressure** | | | | | |
| Adjusted r^2 | 0.00 | 0.13 | 0.00 | 0.00 | 0.16 |
| Correlation Coefficient | -0.06 | -0.49 | -0.10 | -0.23 | -0.51 |

* Correlation coefficients that are significant at the 0.05 level are shown in **bold** type, those significant at the 0.01 level are shown in ***bold italics.***

**Table 21. Correlation matrices for performance characteristics.**

| Material | Adhesion/Erosion | Adhesion/Porosity | Erosion/Porosity |
|---|---|---|---|
| Material 1 (Zn:Al 85:15) | 0.08 | -0.50 | 0.03 |
| Material 2 (Al) | 0.28 | ***-0.59*** | -0.49 |
| Material 3 (Zn) | -0.28 | -0.20 | 0.39 |
| Material 4 (Zn/Al 85:15 Pseudo) | -0.47 | -0.15 | 0.31 |
| Material 5 ($Al/AlO_2$ 90:10) | ***-0.69*** | -0.16 | 0.33 |

### Regression Analysis for Erosion Data

- *Erosion and angle* — No material shows significant correlation for this regression pair. The $r^2$ values suggest that the regression does not adequately predict variation in erosion data with changing angles of the gun. This result draws into question any dependence on suggested angle of gun positions derived from the Taguchi models.
- *Erosion and distance* — Only materials 3 and 4 show a strong correlation (significant at the <0.01 level) for this regression, associated $r^2$ values are 0.6 or greater. Together the dimensions and vector of these regressions are consistent with the results of the modeling exercises. Where there is a low p coefficient in both the Y and the S models, there is a strong regression coefficient. Such is the case with materials 3 and 4. The vector of these correlation coefficients is consistent with the predicted low distance to sample, to reduce erosion weight loss.
- *Erosion and power* — The regression coefficients for this variable pairing are insignificant. This result is consistent with the general trends observed in the Y model (though material 3 showed a very low p coefficient in the S model).
- *Erosion and pressure* — The regression coefficients for this variable pairing are insignificant. This is consistent with the low p coefficients found in both the Y and S models for all materials.

### Regression Analysis for Porosity and Oxide Data

- *Porosity and angle* — Only for material 3 (Zn) is a significant correlation coefficients seen (<0.01 level) for this variable pairing. The $r^2$ value is 0.54, which indicates that the regression accounts for the variability in just over half of the data. The negative value of all correlation coefficients suggests that higher angles (closer to 90 degrees) will lower porosity, which is surprising given the predicted low optimum settings for angle of the gun to minimize porosity in the Y models. This inconsistency is consistent with a general trend of the study — an inability to correctly predict the influence of angle of gun on the performance of the applied thermal spray materials.
- *Porosity and all other parameters* — No significant correlations nor high $r^2$ values are seen for any material for any other variable pairing.

### Correlation Between Performance Characteristics

Table 21 lists the correlation matrices for all three performance factors for each material.

Material 1, which is a frequently specified thermal spray material, shows a statistically significant correlation between porosity and adhesion. The negative sign of the correlation coefficient indicates that lower porosity will tend to result in higher adhesion. The magnitude of the coefficient is low (0.50) indicating a weak degree of correlation. Materials 2 and 5 show high statistically significant correlations between erosion weight loss and adhesion. The correlation coefficient is negative, so lower erosion weight losses correspond to higher observed adhesion strength. Material 4 shows similar correspondence between erosion weight loss and observed adhesion. These correlation coefficients range from 0.47 to 0.69, indicative of a weak to moderate degree of correlation.

# 4 Conclusions and Recommendations

## General

### *Primary Factors Influencing Applied Material Performance for All Materials*

The generally accepted application parameters for all materials are those suggested as "center-point" values. These values are: distance to the sample (12 in.); power to the gun (375 amps); pressure at the gun (90 psi); and angle to the sample surface (90 degrees). The influence that variations in these parameters can have in deciding performance is important to ensuring a cost-effective thermal spray metallizing application. Whether there is a need to suggest changes to the accepted application parameters depends on the degree to which a parameter affects material performance.

To determine if the accepted application procedures also ensured needed performance characteristics, a series of modeling exercises were conducted based on an experimental design using a Taguchi L9 matrix. Fifteen of these matrices were modeled: one each for every material to examine each of the three performance characteristics of interest: adhesion, erosion resistance, and porosity and oxide content.

### *Best Approach for Metallizing (All Studied Materials)*

These modeling exercises support a change to the accepted production parameters for metallizing. The modeling suggests that a lower distance from gun to the surface (6 in.) distance is optimum. This conclusion should be subjected to re-evaluation to confirm the validity of the Taguchi model output. No other changes to the generally accepted application parameters are supported by the modeling exercises.

## Comparison of Performance of Materials at Selected Parameter Levels (Center-Point Values)

Table 22 compares the performance of the 5 materials evaluated under this project for the 12 center-point samples that constituted the outer array. The conditions of application used for preparing these samples are those which the manufacturer typically recommends.

***Adhesion*** **-** The Al or Al alloys show significantly higher adhesion than the Zn:Al alloys show. Conversely, the pure zinc samples show the lowest adhesion of all materials. The adhesion results showed the greatest precision among the three tests. Coefficients of variation range from 3 to 8 percent.

***Erosion*** **-** There is little to choose between the mean values of erosion weight loss shown by the samples of Zn:Al or Al alloys. Pure zinc samples do show higher overall weight losses than any other material. The coefficient of variation in weight loss is highest for the Zn:Al alloy (material 1). Because of the low overall precision, any effects on erosion weight loss should be interpreted with caution.

***Porosity*** **-** Porosity of these outer array samples is very close for materials 1 through 3. Material 4 shows a higher tendency to porosity and oxide defects, exceeded only by material 5. The base formula for material 5 already includes 10% $AlO_2$, which contributes to its high level of porosity (0.24). The material with the lowest overall variability in porosity is material 5, while material 2 has the highest overall variability in porosity.

Overall material 1 (standard Zn:Al alloy) compared favorably with materials 3, 4, and 5. Material 1 has the best (or tied for best) performance for erosion and porosity. The adhesion is around 38 to 40 percent less than that for the Al or Al:$AlO_2$ materials. The material having comparable overall performance is aluminum, which is also widely specified for corrosion control applications. A discussion of how these materials compare under the varying conditions of distance, angle, power, and pressure follows.

**Table 22. Comparing alternate materials using center-point values.**

| Material: | 1 | 2 | 3 | 4 | 5 |
|---|---|---|---|---|---|
| Property | Zn:Al 85:15 | Aluminum | Zinc | Zn:Al (85:15) Pseudo Alloy | Al:$AlO_2$ (90:10) |
| ***Adhesion*** | | | | | |
| Mean | 1134 | 1761 | 803 | 1362 | 1855 |
| Std. Dev. | 67 | 141 | 48 | 37 | 99 |
| Coeff. of Var. | 0.06 | 0.08 | 0.06 | 0.03 | 0.05 |
| ***Erosion*** | | | | | |
| Mean | 0.05 | 0.05 | 0.08 | 0.06 | 0.05 |
| Std. Dev. | 0.04 | 0.00 | 0.01 | 0.01 | 0.00 |
| Coeff. of Var. | 0.78 | 0.05 | 0.11 | 0.12 | 0.04 |
| ***Porosity*** | | | | | |
| Mean | 0.09 | 0.11 | 0.09 | 0.16 | 0.24 |
| Std. Dev. | 0.02 | 0.03 | 0.02 | 0.03 | 0.02 |
| Coeff. of Var. | 0.18 | 0.24 | 0.17 | 0.16 | 0.10 |

## Summary of Effects of Parameters on Performance (Taguchi Modeling)

Table 23 summarizes the data for the optimum settings using the Y model (maximizes or minimizes the mean value), the S model (minimizes the variation), and the ANOM (maximizes or minimizes the mean value). The first column presents the mean value (from the L9 matrix data points) and the maximum (for adhesion) or minimum (for erosion and porosity) predicted value based on optimization of the application parameters. In those instances where the coefficient of variation is statistically significant ($P \leq 0.05$), these coefficients are also listed. This discussion will only address rows in which the model yields statistically significant results for the Y or S model.

For material 1, both adhesion and porosity are optimized at a gun distance of 6 in.; however, the porosity variance is minimized (greater precision) at 10 in. The porosity is also optimized at an angle of 86 degrees and a power of 300 amps. For each of these, the ANOM is consistent with 6 in. and 300 amps.

For material 2, the adhesion and porosity are optimized at an angle of 45 degrees (an anomaly discussed previously) and a power of 450 amps.

For material 3, the adhesion, erosion, and porosity are all optimized at 6 in., although the variability for adhesion is minimized at 16 in. There is also inconsistency in optimization of erosion with angle and adhesion with pressure.

**Table 23. Optimizing application variables for coating performance (Taguchi modeling).**

| Parameters | | Distance | | Angle | | Power | | Pressure | |
|---|---|---|---|---|---|---|---|---|---|
| **Material and Property** | | **Coeff** | **Setting** | **Coeff** | **Setting** | **Coeff** | **Setting** | **Coeff** | **Setting** |
| Material 1 | | | | | | | | | |
| Adhesion | Y Model | **-194.6** | **6** | | 68 | | 300 | **46.19** | **70** |
| Maximum | S Model | | 18 | | 64 | | 300 | | 70 |
| 1434 psi | ANOM | | 6 | | 68 | | 375 | | 90 |
| Erosion | Y Model | | 6 | | 81 | | 300 | | 76 |
| Minimum | S Model | | 12 | | 78 | | 340 | | 70 |
| 0.05 g | ANOM | | 6-18 | | 68-90 | | 300 | | 80 |
| Porosity | Y Model | **0.0261** | **6** | **-0.0267** | **86** | **0.0144** | **300** | | 70 |
| Minimum | S Model | **0.009** | **10** | | 69 | **0.009** | **300** | | 70 |
| 0.08 | ANOM | | 6 | | 68-90 | | 300 | | 90 |
| Overall | | | | | | | | | |
| Material 2 | | | | | | | | | |
| Adhesion | Y Model | | 6 | **-94.7** | **45** | **300.7** | **450** | | 70 |
| Maximum | S Model | | 12 | | 72 | | 345 | | 70 |
| 2484 psi | ANOM | | 6 | | 45 | | 450 | | 70 |
| Erosion | Y Model | **0.0031** | **6** | **-0.0024** | **45** | **-0.0046** | **450** | | 70 |
| Minimum | S Model | | 12 | | 78 | | 340 | | 70 |
| 0.04 g | ANOM | | 6 | | 67.5 | | 450 | | 90 |
| Porosity | Y Model | | 6 | | 45 | | 351 | | 70 |
| Minimum | S Model | | 12 | | 45 | | 300 | | 70 |
| 0.14 | ANOM | | 6-18 | | 68 | | 375 | | 70-90 |
| Overall | | | | | | | | | |
| Material 3 | | | | | | | | | |
| Adhesion | Y Model | **-170** | **6** | | 45 | | 387 | **43.5** | **85** |
| Maximum | S Model | **-15.3** | **16** | | 45 | | 300 | **1.79** | **70** |
| 1177 psi | ANOM | | 6 | | 68 | | 375-450 | | 80-90 |
| Erosion | Y Model | **0.0303** | **6** | **-0.0225** | **82** | | 300 | **-0.001** | **70** |
| Minimum | S Model | **-0.002** | **6** | **0.004** | **45** | **-0.003** | **300** | **-0.001** | **70** |
| 0.11 g | ANOM | | 6 | | 68 | | 300-375 | | 90 |
| Porosity | Y Model | **0.0217** | **6** | **-0.0294** | **90** | | 313 | | 70 |
| Minimum | S Model | **0.012** | **6** | | 66 | | 300 | | 70 |
| 0.05 | ANOM | | 6 | | 68 | | 300-450 | | 70-90 |
| Overall | | | | | | | | | |
| Material 4 | | | | | | | | | |
| Adhesion | Y Model | **-114.4** | **6** | | 71 | **32.1** | **450** | | 70 |
| Maximum | S Model | | 12 | | 45 | | 300 | | 80 |
| 1566 psi | ANOM | | 6 | | 90 | | 450 | | 70-90 |
| Erosion | Y Model | **0.0122** | **6** | | 45 | | 421 | | 70 |
| Minimum | S Model | **0.004** | **6** | | 90 | | 302 | | 71 |
| 0.06 g | ANOM | | 6 | | 68 | | 375-450 | | 90 |
| Porosity | Y Model | | 11 | | 74 | | 450 | | 82 |
| Minimum | S Model | | 6 | | 65 | | 361 | | 70 |
| 0.16 | ANOM | | 12 | | 90 | | 375-450 | | 80 |
| Overall | | | | | | | | | |
| Material 5 | | | | | | | | | |
| Adhesion | Y Model | | 6 | **-118.4** | **45** | **107.5** | **450** | | 80 |
| Maximum | S Model | **94.6** | **10** | **72.8** | **62** | | 450 | | 70 |
| 2544 psi | ANOM | | 6 | | 45 | | 450 | | 80 |
| Erosion | Y Model | **0.0057** | **6** | **0.0027** | **45** | **-0.0012** | **390** | **-0.0047** | **84** |
| Minimum | S Model | | 6 | | 45 | | 450 | | 70 |
| 0.02 g | ANOM | | 6 | | 45 | | 375-450 | | 80-90 |
| Porosity | Y Model | | 6 | | 45 | | 382 | | 83 |
| Minimum | S Model | **0.028** | **10** | **-0.002** | **45** | | 300 | **-0.026** | **84** |
| 0.18 | ANOM | | 6-18 | | 68 | | 375-450 | | 80 |
| Overall | | | | | | | | | |

For material 4, the erosion (Y and S models) and the adhesion are optimized at 6 in., the adhesion is also optimized at 450 amps.

For material 5, the Y model recommends 6 in. distance for erosion; whereas, the S model recommends 10 in. for minimizing variance for both adhesion and porosity. For angle, the Y model recommends 45 degrees for both adhesion and erosion, but the S model is inconsistent with these. For power, the recommended adhesion maximum is at 450 amp; whereas, the minimum erosion is predicted for 390 amps. A pressure of 84 psi is recommended by the Y model for erosion and by the S model for porosity.

These data show that the preferred settings for the appropriate parameters are not necessarily consistent among the models and the performance parameters. Thus, it is necessary to consider the sensitivity of the value of the application parameters and the relative importance of the three performance measures in deciding how to use these results.

## Summary of Effect on Adhesion — Abrasive and Surface Profile

With the exception of material 4, the typical effect of abrasive and profile is as follows:

***Abrasive -*** An angular mineral abrasive increases adhesion.

***Surface Profile -*** A deeper profile increases adhesion.

The combined effects of a mineral abrasive with a deep profile results in as much as a ten-fold increase in adhesion, over a small round metallic abrasive (steel shot). Material 4 exhibits anomalous behavior in providing higher adhesion with a metallic (steel shot) abrasive, though it does share the common characteristic of improved adhesion with a deeper profile.

## Summary of Regression and Correlation Analyses

### *Regression Analysis*

Regression between a dependent variable (e.g., adhesion) and an independent variable (e.g., distance) is a measure of how closely the changes in the dependent variable follow the changes in the independent variable. For most of the pairs of variables compared, the regression was not statistically significant (though there

was some dependence). For all but a few, the degree of regression was low ($r^2 <$ 0.5 [less than 50 percent of the regression due to the independent variable]). These exceptions were:

- adhesion vs. distance for materials 1, 3, and 4
- adhesion vs. power for material 2.

Adhesion, therefore, is significantly affected by the distance and power in a consistent and significant manner for these materials.

The absence of significant regression for the other pairs indicates one or more of the following:

- the effect of the independent variable is small
- the effect of the variable is not consistent (e.g., does not change linearly as power or pressure is increased)
- the results are confounded by interaction (e.g., porosity increases with power for one angle but decreases with power for another angle).

### *Correlation Analysis*

Comparisons were also made between different performance parameters, including adhesion-erosion, adhesion-porosity, and erosion-porosity. The data indicate that there are significant but weak correlations between erosion and adhesion for materials 1, 3, 4, and 5, but very low correlation between adhesion and porosity and between erosion and porosity. This result indicates that, in optimizing the application parameters, it may be necessary to choose one performance parameter to optimize over another. For example, from Table 23 for material 5, adhesion is maximized if the pressure is 85 psi whereas for minimum porosity the optimum setting is 70 psi.

The regression analysis showed strong interdependence between variables (such as distance, angle, power, and pressure) and measured performance (adhesion, erosion, and porosity) in the expected manner for all pairings except the following:

- Adhesion and angle
- Erosion and angle
- Porosity and angle.

In summary, the regression analysis validated the integrity of the modeling exercise, except where angle was the application variable. This lack of validation for

the portion of the models involving varying of angle provides justification to ignore the unusual application settings for angle of the gun shown earlier in Table 23.

## Recommendations

### *Application Parameters for Material 1 (85:15 Zn:Al Alloy)*

Suggested application parameters for this material are as follows:

- Distance to the surface — 6 to 10 in.
- Angle of gun — 90 degrees
- Power to the gun — 300 amps
- Pressure at the gun — 90psi.

From Table 23, the maximum adhesion predicted by optimizing application settings is 1,434 psi. This figure is a moderate increase over the mean adhesion of 1,134 psi observed under standard conditions. Similarly, optimized porosity is predicted to improve from the mean value of 0.09 (9 percent) obtained under standard conditions to 0.08 (8 percent). Optimizing application settings does not improve erosion from that observed with samples prepared under standard conditions.

### *Application Parameters for Alternate Materials*

#### Material 2 - Aluminum

- Distance to the surface — 6 to 11 in.
- Angle of gun — 90 degrees
- Power to the gun — 450 amps
- Pressure at the gun — 90 psi

#### Material 3 - Zinc

- Distance to the surface — 6 in.
- Angle of gun — 90 degrees (unless a re-evaluation of the suggested settings confirms the given lower values)
- Power to the gun — 400 amps
- Pressure at the gun — 90 psi

#### Material 4 - Zn:Al (85:15) Pseudo Alloy

- Distance to the surface — 6 in.
- Angle of gun — 90 degrees
- Power to the gun — 350-400 amps
- Pressure at the gun — 80 to 90 psi

#### Material 5 - Al:$AlO_2$ (90:10) Alloy

- Distance to the surface — 6 to 10 in.
- Angle of gun — 90 degrees
- Power to the gun — 390 amps
- Pressure at the gun — 80 to 90 psi

#### Comparisons With Material 1

Overall, material 1 (85:15 Zn:Al alloy) compared favorably with materials 3, 4, and 5. Material 1 has the best (or tied for best) performance for erosion and porosity. Adhesion is approximately 38 to 40 percent less than that for the Al or Al:$AlO_2$ materials (materials 2 and 5, respectively). One material having comparable overall performance to material 1 is Al (material 2). This material is also widely specified for corrosion control applications.

### *Performance Evaluation Procedures*

Three performance evaluation procedures were featured in this study:

- measurement of pull-off adhesion strength
- determination of cavitation erosion resistance
- assessment of porosity and oxide content through image analysis.

### *Measurement of Pull-Off Adhesion Strength*

This procedure was used for two different aims. First, it was the only performance attribute measured for a branch experiment that sought to determine whether adhesion was influenced by the type (shape) of abrasive and the depth of profile created. Second it was one of the three performance attributes used in the statistical modeling exercises to determine optimum application conditions. All adhesion testing was done in accordance with ASTM D4541. Adhesion testing proved a useful way to distinguish the relative influence of abrasive shape and profile created on achieved adhesion.

### *Determination of Cavitation Erosion Resistance*

The procurement called for cavitation erosion testing in accordance with ASTM G32. Researchers deviated from this standard practice for the following reasons:

- ASTM G32 calls for application of thin samples of coatings to titanium buttons. These are then directly incorporated into the transducer head of the ultrasonic apparatus. The current study called for thermal spray application onto carbon steel plate for all samples.
- Consultation with manufacturers of the equipment used for the cavitation erosion test and volunteer technical representatives from the ASTM technical committee responsible for the standard stated that:
  1. The mass of any carbon steel button was too great to permit direct attachment to the ultrasonic transducer.
  2. Thermal spray coatings would likely erode completely from the surface of either a carbon steel or titanium button with such direct attachment in a fraction of the time of exposure suggested in the standard.
- Thus, a revision to the method was developed in which coated carbon steel buttons were placed at a uniform close distance from the ultrasound transducer tip for a period of 15 minutes. Despite these precautions, some of the samples underwent near total removal of the thermal spray coating. Because the method deviates from that described in the standard, the results in this report are not of use for interlaboratory comparisons with groups that rigidly employ the ASTM G32 procedure.

### *Assessment of Porosity and Oxide Content Through Image Analysis*

The image analysis and quantification procedure was based on the use of DIC microscopy. For materials 1 through 4, this yielded the expected result of high quality images taken from samples prepared using traditional metallographic polishing techniques. It was always possible to obtain an image of the applied metal layer with clear distinction between pore and oxide and the surrounding intact metal layers. Material 5 (the Al:$AlO_2$ alloy) did not yield such high quality images. The lower quality is believed to be due, in part, to the high intrinsic oxide content of the samples. Problems with image acquisition from material 5 were also worsened by the extremely poor film quality of the applied samples. This observation is in keeping with the records from the preparation of the bulk samples. All other materials applied with relatively few problems, while material 5 was observed to undergo noticeable “burning” in the plasma as particles traveled to the surface. This burning resulted in visible dark inclusions on the surfaces of the samples.

Quantification of the images depended on the quality of the acquired images. The images for materials 1 through 4 required infrequent special treatment. Almost every one of the material 5 samples underwent editing prior to thresholding and binary conversion as described earlier.

### *Additional Research*

In the earlier discussion of Taguchi modeling, a four-step diagram was used to describe the process. This study completed three of those steps. It is strongly recommended that the fourth step be completed by confirming the results through re-testing. It is suggested that this additional testing focus on the confirmation of the suggested application conditions to enhance performance and minimize applied coating variation. A well-designed branch experiment in which the default application angle is truly the center-point value in an orthogonal array is also suggested to clarify the role that angle of the gun plays (if any) in determining performance.

The results from this research also suggest that some of the commonly used means to assess coating performance in the field are of doubtful value to an inspector. Specifically, adhesion is a widely used test to determine adequacy of applied thermal spray films. Our testing work confirms that adhesion will distinguish between a well-prepared surface and a poorly prepared surface. Adhesion results for thermal spray materials applied under very poor conditions are surprisingly high, once surface preparation is optimized. This suggests that adhesion results are not a good predictor of physical performance for these materials. As an alternative to using adhesion alone as a measure of applied thermal spray metal integrity, it is suggested that the Corps of Engineers examine development of a procedure, amenable to field use, which can estimate porosity and oxide content. Finally, the results presented in this report are technical and scientific in nature. It is suggested that a simple guide be developed for specifiers, engineers, and inspectors to present the import of these results in layman's terms.

### *Statistical Modeling*

Overall, the statistical modeling exercises provided considerable value to this project. The structured experimental design and analytical approach simplified understanding of the importance of key application parameters while holding expenses in check. The primary recommendation regarding statistical modeling is to limit the number of center-point specimens used in any future design. It seems that the same amount of effort could have been expended to double the design to a Taguchi L18 matrix, substantially increasing the validity of the data obtained.

The one puzzling aspect from the statistical modeling activities are the odd suggested levels for the angle of the gun. This result may be related to the use of the L9 matrix in which no repeat samples are run. A pair of samples, each having adequate performance characteristics, though applied at less than optimum angles, can greatly influence the model output. Another interpretation is that the measured performance of the metal coatings is not truly sensitive to the angle of the gun.

# References

American Society for Testing and Materials (ASTM) G32, “Standard Test Method for Cavitation Erosion Using Vibratory Apparatus.”

ASTM D4285, “Test Method for Indicating Oil or Water in Compressed Air.”

ASTM D4417, “Test Methods for Field Measurement of Surface Profile of Blast Cleaned Steel,” method C (replica tape).

ASTM D4541, “Standard Test Method for Evaluating the Pull Off Strength of Coatings Using Portable Adhesion Testers.”

ASTM E691, “Practice for Conducting an Interlaboratory Study to Determine the Precision of a Test Method.”

Schwetzke, R., and H. Kreye, “Cavitation Erosion of HBOF Coatings,” in *Thermal Spray - Practical Solutions for Engineering Problems*, 9th National Thermal Spray Conference (ASM International, October 1996).

# Appendix A: Dry-Film Thickness Readings

The tables in this appendix show dry-film thickness readings for each material.

**Table A1. Zn:Al 85/15 (16 +/- 2 mils) dry-film thickness readings.**

| Specimen No. | DFT Average (mils) | DFT Low (mils) | DFT High (mils) |
|---|---|---|---|
| 1 | 15.7 | 14 | 15.8 |
| 2 | 14 | 13 | 16.1 |
| 3 | 14.7 | 14 | 16.1 |
| 4 | 15.9 | 15.2 | 16.4 |
| 5 | 18.4 | 17.2 | 19.3 |
| 6 | 15.8 | 15.3 | 16.7 |
| 7 | 15.6 | 14.1 | 16.6 |
| 8 | 13.7 | 12.9 | 14.7 |
| 9 | 16.3 | 15.4 | 16.9 |
| 10 | 17.4 | 16.4 | 18.1 |
| 11 | 14 | 13 | 15 |
| 12 | 15.1 | 14.2 | 15.7 |
| 13 | 15.3 | 14.3 | 16.7 |
| 14 | 15.8 | 14.7 | 16.4 |
| 15 | 15.7 | 15.1 | 16.8 |
| 16 | 15.4 | 14.5 | 16.1 |
| 17 | 14.5 | 14.6 | 16.4 |
| 18 | 15.2 | 14.5 | 15.8 |
| 19 | 15.7 | 14.9 | 16.6 |
| 20 | 15.4 | 14 | 16.8 |
| 21 | 15.7 | 14.2 | 16.8 |

**Table A2. Aluminum (10 +/- 2 mils) dry-film thickness readings.**

| Specimen No. | DFT Average (mils) | DFT Low (mils) | DFT High (mils) |
|---|---|---|---|
| 22 | 9.8 | 7.9 | 12.1 |
| 23 | 9.9 | 8.7 | 12.3 |
| 24 | 10.5 | 8.8 | 13.8 |
| 25 | 10.2 | 8.6 | 13.4 |
| 26 | 9.4 | 7.2 | 11.1 |
| 27 | 10.7 | 9.5 | 14.2 |
| 28 | 11.5 | 10.2 | 13.5 |
| 29 | 8.7 | 8.1 | 10 |
| 30 | 11.5 | 9.8 | 14.1 |
| 31 | 12.1 | 10.6 | 13.1 |
| 32 | 11.9 | 10.7 | 12.8 |
| 33 | 11.5 | 10.5 | 14.3 |
| 34 | 11.1 | 10.5 | 13.8 |
| 35 | 12.1 | 10.6 | 13.3 |
| 36 | 11.9 | 11 | 12.9 |
| 37 | 12.5 | 10.6 | 14.3 |
| 38 | 12.1 | 10.3 | 13.3 |
| 39 | 11.4 | 10.3 | 13.2 |
| 40 | 11.7 | 10.4 | 13.3 |
| 41 | 12.2 | 10.5 | 14.8 |
| 42 | 12.6 | 10.7 | 15.8 |

**Table A3. Zinc (16 +/- 2 mils) dry-film thickness readings.**

| Specimen No. | DFT Average (mils) | DFT Low (mils) | DFT High (mils) |
|---|---|---|---|
| 43 | 16.2 | 14.8 | 18.6 |
| 44 | 14.9 | 13 | 16.4 |
| 45 | 14.3 | 13.8 | 14.8 |
| 46 | 14.4 | 13.2 | 15.6 |
| 47 | 16.3 | 14.5 | 17.6 |
| 48 | 14 | 13.2 | 15.5 |
| 49 | 16 | 14.5 | 17.3 |
| 50 | 15.3 | 13.8 | 16.8 |
| 51 | 16.8 | 15.1 | 18.1 |
| 52 | 16.2 | 15.2 | 17.2 |
| 53 | 14.3 | 13.2 | 15.9 |
| 54 | 16.4 | 15.5 | 17.7 |
| 55 | 16.4 | 15.1 | 17.6 |
| 56 | 16.2 | 15.1 | 17.2 |
| 57 | 16.3 | 15.1 | 17.8 |
| 58 | 16.5 | 15.4 | 17.3 |
| 59 | 16.3 | 14.5 | 18.1 |
| 60 | 16 | 15 | 16.9 |
| 61 | 16.3 | 15.2 | 17.1 |
| 62 | 16 | 14.6 | 17.5 |
| 63 | 16.6 | 15.1 | 18 |

**Table A4. Zn:Al 85:15 pseudo alloy (16 +/- 2 mils) dry-film thickness readings.**

| Specimen No. | DFT Average (mils) | DFT Low (mils) | DFT High (mils) |
|---|---|---|---|
| 64 | 15.6 | 14.5 | 16.6 |
| 65 | 15 | 12.8 | 16.8 |
| 66 | 16.4 | 15.3 | 18.5 |
| 67 | 14.8 | 14.3 | 17.5 |
| 68 | 16.4 | 15.4 | 17.5 |
| 69 | 14.3 | 13.6 | 15.5 |
| 70 | 14.3 | 13.5 | 17.3 |
| 71 | 14.6 | 13.6 | 16 |
| 72 | 14.9 | 13.6 | 16.6 |
| 73 | 15.8 | 15.3 | 16.7 |
| 74 | 15.9 | 14.6 | 17.9 |
| 75 | 16.1 | 15.1 | 17.5 |
| 76 | 15.4 | 13.7 | 17.3 |
| 77 | 15.5 | 14.7 | 16.8 |
| 78 | 16.1 | 15.3 | 17.3 |
| 79 | 15.9 | 14.9 | 16.7 |
| 80 | 18.2 | 17.2 | 18.7 |
| 81 | 15.1 | 13.7 | 15.9 |
| 82 | 15.1 | 14.3 | 16.2 |
| 83 | 14.5 | 13.6 | 16.3 |
| 84 | 15.5 | 14.6 | 16.5 |

**Table A5. Al/$AlO_2$ 90/10 (10 +/- 2 mils) dry-film thickness readings.**

| Specimen no. | DFT average (mils) | DFT Low (mils) | DFT High (mils) |
|---|---|---|---|
| 85 | 9.8 | 8.2 | 13.7 |
| 86 | 8.5 | 7 | 13.4 |
| 87 | 8.6 | 6.9 | 10 |
| 88 | 9.6 | 8 | 11.7 |
| 89 | 13.1 | 11.5 | 15.9 |
| 90 | 10.7 | 9.5 | 13.9 |
| 91 | 9.5 | 8.1 | 11.9 |
| 92 | 10.2 | 8.1 | 13 |
| 93 | 10.8 | 9.5 | 12.5 |
| 94 | 11.2 | 9 | 12.9 |
| 95 | 11 | 9.2 | 13.6 |
| 96 | 11.8 | 10.3 | 14.5 |
| 97 | 11.9 | 10.4 | 13.7 |
| 98 | 11.6 | 10.2 | 13.8 |
| 99 | 11.1 | 9.1 | 12.5 |
| 100 | 11.3 | 9.7 | 14.8 |
| 101 | 11.9 | 9.8 | 14.8 |
| 102 | 12.9 | 10 | 16.8 |
| 103 | 11.3 | 10.6 | 14.8 |
| 104 | 12.2 | 10.3 | 14.2 |
| 105 | 11.6 | 9.8 | 14.7 |

**Table A6. Samples prepared for determination of influence of surface preparation on adhesion.**

| Specimen No. | DFT Average (mils) | DFT Low (mils) | DFT High (mils) |
|---|---|---|---|
| Zn:Al 85:15 (16 +/- 2 mils) | | | |
| 106 | 15.7 | 14.9 | 16.6 |
| 107 | 15.7 | 14.8 | 16.3 |
| 108 | 16.3 | 15.3 | 17.1 |
| 109 | 14.7 | 13.6 | 15.5 |
| Aluminum (10 +/- 2 mils) | | | |
| 110 | 12.5 | 10.4 | 14.3 |
| 111 | 12.6 | 11.2 | 13.5 |
| 112 | 12.6 | 10.9 | 15 |
| 113 | 11.9 | 10.5 | 14.8 |
| Zinc (16 +/- 2 mils) | | | |
| 114 | 16.4 | 15.8 | 17.1 |
| 115 | 15.6 | 15.4 | 17.2 |
| 116 | 17 | 15.8 | 18.1 |
| 117 | 16.2 | 15.2 | 17.1 |
| Zn:Al 85:15 Pseudo (16 +/- 2 mils) | | | |
| 118 | 15.4 | 14.6 | 17.4 |
| 119 | 14.8 | 13.7 | 15.6 |
| 120 | 15.2 | 14.1 | 17.2 |
| 121 | 15 | 13.9 | 16.5 |
| Al:$AlO_2$ 90:10 Alloy (10 +/- 2 mils) | | | |
| 122 | 11.9 | 10.3 | 13.8 |
| 123 | 12.4 | 11.1 | 13.6 |
| 124 | 11.3 | 9.8 | 13.3 |
| 125 | 11.1 | 9.3 | 14.4. |

# Appendix B: Adhesion Pull-Off Strength Results

The tables in this appendix show the tensile pull-off adhesion strength readings for all materials.

**Table B1. Adhesion pull-off results for Zn:Al (85:15) alloy.**

| Specimen Number | Adhesion Test Results (psi pulloff) | | | | |
|---|---|---|---|---|---|
| | A | B | C | D | E |
| 001 | 1508 | 1345 | 1386 | 1182 | 1345 |
| 002 | 1467 | 1345 | 1467 | 1304 | 1141 |
| 003 | 1549 | 1549 | 1590 | 1508 | 1549 |
| 004 | 1182 | 1263 | 1263 | 1182 | 1141 |
| 005 | 1223 | 1100 | 1100 | 1141 | 1223 |
| 006 | 1263 | 1304 | 1182 | 1182 | 1182 |
| 007 | 1018 | 1018 | 978.1 | 937.3 | 1018 |
| 008 | 1100 | 1141 | 1018 | 1018 | 1018 |
| 009 | 1100 | 1018 | 1018 | 1059 | 937.3 |
| 010 | 1263 | 1263 | 1304 | 1263 | 1263 |
| 011 | 1304 | 1182 | 1263 | 1059 | 1223 |
| 012 | 1100 | 1100 | 1223 | 1182 | 1141 |
| 013 | 1263 | 1182 | 1223 | 1223 | 1161 |
| 014 | 1202 | 1243 | 1120 | 1120 | 1080 |
| 015 | 1141 | 1100 | 1120 | 1141 | 1080 |
| 016 | 1080 | 1080 | 1100 | 1120 | 1080 |
| 017 | 1100 | 1039 | 1059 | 1018 | 1080 |
| 018 | 998.5 | 1059 | 1039 | 1080 | 1080 |
| 019 | 1120 | 1161 | 1100 | 1141 | 1059 |
| 020 | 1223 | 1141 | 1059 | 998.5 | 1039 |
| 021 | 1120 | 1059 | 1120 | 1120 | 1039 |

**Table B2. Adhesion pull-off results for Al.**

| Specimen Number | Adhesion Test Results (psi pulloff) | | | | |
|---|---|---|---|---|---|
| | A | B | C | D | E |
| 022 | 1711 | 1670 | 1956 | 2038 | 2038 |
| 023 | 2079 | 1834 | 1793 | 2038 | 1670 |
| 024 | 2201 | 2242 | 1997 | 2160 | 2038 |
| 025 | 2039 | 2018 | 2039 | 2039 | 2039 |
| 026 | 1997 | 2446 | 2364 | 2201 | 2201 |
| 027 | 1425 | 1548 | 1507 | 1507 | 1303 |
| 028 | 1793 | 2568 | 2446 | 2568 | 2405 |
| 029 | 1589 | 1548 | 1548 | 1670 | 1548 |
| 030 | 1997 | 1752 | 1752 | 1874 | 1956 |
| 031 | 1670 | 1670 | 1752 | 1752 | 1874 |
| 032 | 1425 | 936.1 | 1834 | 1670 | 1548 |
| 033 | 1670 | 1630 | 1548 | 1711 | 1589 |
| 034 | 1672 | 1814 | 1876 | 1814 | 1243 |
| 035 | 1835 | 1937 | 1937 | 1998 | 1855 |
| 036 | 1876 | 1916 | 1529 | 1896 | 1794 |
| 037 | 1978 | 1978 | 1956 | 1937 | 1774 |
| 038 | 1998 | 1835 | 1916 | 1794 | 1957 |
| 039 | 1916 | 1733 | 1835 | 1855 | 1835 |
| 040 | 1855 | 1774 | 1855 | 1733 | 1733 |
| 041 | 1794 | 1876 | 1835 | 1937 | 1814 |
| 042 | 1325 | 1508 | 1672 | 1529 | 1869 |

**Table B3. Adhesion pull-off results for Zn.**

| Specimen Number | Adhesion Test Results (psi pulloff) | | | | |
|---|---|---|---|---|---|
| | A | B | C | D | E |
| 043 | 957.7 | 1039 | 1018 | 1059 | 1039 |
| 044 | 1141 | 1080 | 1263 | 1182 | 1263 |
| 045 | 1100 | 1100 | 1202 | 1120 | 1182 |
| 046 | 957.7 | 896.5 | 896.5 | 896.5 | 957.7 |
| 047 | 876 | 814.8 | 814.8 | 814.8 | 814.8 |
| 048 | 855.6 | 855.6 | 896.5 | 855.6 | 896.5 |
| 049 | 794.4 | 774 | 814.8 | 794.4 | 814.8 |
| 050 | 794.4 | 814.8 | 814.8 | 774 | 753.6 |
| 051 | 753.6 | 733.2 | 753.6 | 692.4 | 774 |
| 052 | 896.5 | 876 | 814.8 | 876 | 916.9 |
| 053 | 814.8 | 876 | 814.8 | 916.9 | 957.7 |
| 054 | 876 | 835.2 | 814.8 | 794.4 | 937.3 |
| 055 | 733.7 | 754.1 | 723.5 | 733.7 | 743.9 |
| 056 | 682.7 | 825.6 | 764.3 | 743.9 | 682.7 |
| 057 | 784.7 | 866.4 | 764.3 | 713.3 | 754.1 |
| 058 | 795 | 795 | 723.5 | 652.1 | 856.2 |
| 059 | 815.4 | 835.8 | 784.7 | 723.5 | 764.3 |
| 060 | 856.2 | 784.7 | 805.2 | 764.3 | 662.3 |
| 061 | 835.8 | 825.6 | 815.4 | 795 | 733.7 |
| 062 | 886.8 | 835.8 | 835.8 | 815.4 | 784.7 |
| 063 | 815.4 | 846 | 825.6 | 805.2 | 805.2 |

**Table B4. Adhesion pull-off results for Zn:Al (85:15) pseudo alloy**

| Specimen Number | Adhesion Test Results (psi pulloff) | | | | |
|---|---|---|---|---|---|
| | A | B | C | D | E |
| 064 | 1447 | 1447 | 1365 | 1427 | 1508 |
| 065 | 1467 | 1488 | 1406 | 1529 | 1529 |
| 066 | 1529 | 1569 | 1636 | 1712 | 1488 |
| 067 | 1345 | 1467 | 1386 | 1284 | 1365 |
| 068 | 1427 | 1427 | 1467 | 1406 | 1325 |
| 069 | 1325 | 1386 | 1345 | 1345 | 1386 |
| 070 | 1284 | 1223 | 1304 | 1223 | 1243 |
| 071 | 1325 | 1325 | 1223 | 1263 | 1182 |
| 072 | 1406 | 1325 | 1365 | 1161 | 1263 |
| 073 | 1365 | 1325 | 1243 | 1325 | 1325 |
| 074 | 1386 | 1386 | 1325 | 1263 | 1345 |
| 075 | 1325 | 1345 | 1263 | 1243 | 1386 |
| 076 | 1386 | 1345 | 1406 | 1365 | 1263 |
| 077 | 1386 | 1386 | 1386 | 1467 | 1427 |
| 078 | 1386 | 1386 | 1345 | 1325 | 1365 |
| 079 | 1386 | 1365 | 1365 | 1427 | 1345 |
| 080 | 1365 | 1325 | 1427 | 1386 | 1406 |
| 081 | 1325 | 1325 | 1345 | 1263 | 1365 |
| 082 | 1427 | 1365 | 1427 | 1325 | 1284 |
| 083 | 1447 | 1365 | 1447 | 1467 | 1447 |
| 084 | 1345 | 1284 | 1406 | 1386 | 1427 |

**Table B5. Adhesion pull-off results for Al:$AlO_2$ (90:10) alloy.**

| Specimen Number | Adhesion Test Results (psi pulloff) | | | | |
|---|---|---|---|---|---|
| | A | B | C | D | E |
| 085 | 1956 | 2242 | 1997 | 2079 | 2242 |
| 086 | 2079 | 2364 | 1915 | 2691 | 1997 |
| 087 | 2242 | 1956 | 2201 | 2201 | 2079 |
| 088 | 2160 | 2079 | 2160 | 2323 | 1997 |
| 089 | 1915 | 2038 | 1956 | 1997 | 2079 |
| 090 | 1997 | 1956 | 1956 | 2160 | 2201 |
| 091 | 2854 | 1874 | 2283 | 2487 | 2405 |
| 092 | 1956 | 1630 | 650.4 | 2446 | 1874 |
| 093 | 1997 | 1752 | 1793 | 1997 | 1793 |
| 094 | 1956 | 1589 | 1956 | 1711 | 1630 |
| 095 | 1793 | 1997 | 1262 | 1997 | 1752 |
| 096 | 1997 | 1956 | 1915 | 1752 | 1752 |
| 097 | 1956 | 1874 | 1874 | 2201 | 1752 |
| 098 | 2242 | 1874 | 2160 | 1997 | 1548 |
| 099 | 2038 | 2119 | 1834 | 1915 | 2079 |
| 100 | 1752 | 1956 | 1752 | 1915 | 1956 |
| 101 | 1956 | 1956 | 2079 | 1548 | 1670 |
| 102 | 2079 | 1956 | 1956 | 1956 | 1874 |
| 103 | 1793 | 1997 | 1589 | 1956 | 1915 |
| 104 | 1997 | 1425 | 1466 | 1711 | 1793 |
| 105 | 1670 | 1834 | 1834 | 1752 | 1711 |

**Table B6. Adhesion pull-off results for subset of samples to determine effect of surface preparation.**

| Specimen Number | Adhesion Test Results (psi pulloff) | | | | |
|---|---|---|---|---|---|
| | A | B | C | D | E |
| 106 | 998.5 | 1141 | 1018 | 1018 | 978.1 |
| 107 | 1243 | 1202 | 1223 | 1202 | 1182 |
| 108 | 101.1 | 101.1 | 101.1 | 101.1 | 101.1 |
| 109 | 386.8 | 305.2 | 254.1 | 243.9 | 263.8 |
| 110 | 1794 | 1569 | 1590 | 1631 | 1549 |
| 111 | 1794 | 1835 | 1876 | 1876 | 1712 |
| 112 | 1243 | 1039 | 1039 | 978.1 | 1059 |
| 113 | 1080 | 1120 | 932.3 | 1223 | 1039 |
| 114 | 743.9 | 795 | 835.8 | 754.1 | 815.4 |
| 115 | 805.2 | 856.2 | 886.8 | 897 | 866.4 |
| 116 | 101.1 | 101.1 | 111.3 | 121.5 | 101.5 |
| 117 | 101.1 | 101.1 | 111.3 | 101.1 | 101.1 |
| 118 | 1019 | 1039 | 1243 | 1263 | 1284 |
| 119 | 1406 | 1325 | 1386 | 1488 | 1529 |
| 120 | 1835 | 2936 | 650.4 | 2201 | 2405 |
| 121 | 1446 | 3670 | 3670 | 3425 | 3834 |
| 122 | 1651 | 1651 | 1508 | 1712 | 1569 |
| 123 | 1733 | 1937 | 1937 | 1916 | 1876 |
| 124 | 753.6 | 876 | 692.4 | 937.3 | 835.2 |
| 125 | 876 | 743.9 | 825.6 | 795 | 795 |

# Appendix C: Erosion Weight Loss Results

The tables in this appendix show the weight losses (in grams) for all materials.

**Table C1. Cavitation erosion weight losses for Zn:Al (85:15) alloy.**

| Settings | | | | Weight Loss/g | | |
|---|---|---|---|---|---|---|
| Distance (in.) | Angle (°) | Power (amps) | Pressure (psi) | Y1 | Y2 | Y3 |
| 6 | 45 | 300 | 70 | 0.055 | 0.0478 | 0.0403 |
| 6 | 90 | 375 | 80 | 0.031 | 0.0516 | 0.0304 |
| 6 | 67.5 | 450 | 90 | 0.028 | 0.0412 | 0.0387 |
| 12 | 45 | 375 | 90 | 0.045 | 0.0472 | 0.466 |
| 12 | 90 | 450 | 70 | 0.038 | 0.0353 | 0.0369 |
| 12 | 67.5 | 300 | 80 | 0.04 | 0.037 | 0.0486 |
| 18 | 45 | 450 | 80 | 0.031 | 0.059 | 0.03 |
| 18 | 90 | 300 | 90 | 0.048 | 0.042 | 0.0452 |
| 18 | 67.5 | 375 | 70 | 0.057 | 0.0467 | 0.0559 |
| 12 | 90 | 375 | 80 | 0.031 | 0.0508 | 0.0512 |
| 12 | 90 | 375 | 80 | 0.051 | 0.0434 | 0.0524 |
| 12 | 90 | 375 | 80 | 0.048 | 0.0382 | 0.0522 |
| 12 | 90 | 375 | 80 | 0.041 | 0.0497 | 0.4615 |
| 12 | 90 | 375 | 80 | 0.039 | 0.0268 | 0.0285 |
| 12 | 90 | 375 | 80 | 0.045 | 0.0347 | 0.0299 |
| 12 | 90 | 375 | 80 | 0.036 | 0.0493 | 0.0449 |
| 12 | 90 | 375 | 80 | 0.031 | 0.044 | 0.0512 |
| 12 | 90 | 375 | 80 | 0.037 | 0.0407 | 0.0351 |
| 12 | 90 | 375 | 80 | 0.044 | 0.0466 | 0.0486 |
| 12 | 90 | 375 | 80 | 0.054 | 0.0523 | 0.0346 |
| 12 | 90 | 375 | 80 | 0.025 | 0.042 | 0.0219 |

**Table C2. Cavitation erosion weight losses for Al.**

| Settings | | | | Weight Loss/g | | |
|---|---|---|---|---|---|---|
| Distance (in.) | Angle (°) | Power (amps) | Pressure (psi) | Y1 | Y2 | Y3 |
| 6 | 45 | 300 | 70 | 0.037 | 0.0453 | 0.0352 |
| 6 | 90 | 375 | 80 | 0.032 | 0.0294 | 0.0359 |
| 6 | 67.5 | 450 | 90 | 0.028 | 0.031 | 0.0307 |
| 12 | 45 | 375 | 90 | 0.039 | 0.0405 | 0.0363 |
| 12 | 90 | 450 | 70 | 0.029 | 0.0304 | 0.0311 |
| 12 | 67.5 | 300 | 80 | 0.047 | 0.0489 | 0.0463 |
| 18 | 45 | 450 | 80 | 0.031 | 0.0462 | 0.0366 |
| 18 | 90 | 300 | 90 | 0.04 | 0.0387 | 0.0387 |
| 18 | 67.5 | 375 | 70 | 0.04 | 0.0444 | 0.0433 |
| 12 | 90 | 375 | 80 | 0.048 | 0.0539 | 0.053 |
| 12 | 90 | 375 | 80 | 0.057 | 0.0571 | 0.0536 |
| 12 | 90 | 375 | 80 | 0.049 | 0.0565 | 0.0557 |
| 12 | 90 | 375 | 80 | 0.048 | 0.0544 | 0.0481 |
| 12 | 90 | 375 | 80 | 0.05 | 0.0527 | 0.0539 |
| 12 | 90 | 375 | 80 | 0.05 | 0.0514 | 0.0513 |
| 12 | 90 | 375 | 80 | 0.053 | 0.052 | 0.0522 |
| 12 | 90 | 375 | 80 | 0.05 | 0.0498 | 0.052 |
| 12 | 90 | 375 | 80 | 0.049 | 0.0503 | 0.0508 |
| 12 | 90 | 375 | 80 | 0.055 | 0.0526 | 0.052 |
| 12 | 90 | 375 | 80 | 0.053 | 0.0452 | 0.0492 |
| 12 | 90 | 375 | 80 | 0.032 | 0.0539 | 0.0534 |

**Table C3. Cavitation erosion weight losses for Zn.**

| Settings | | | | Weight Loss/g | | |
|---|---|---|---|---|---|---|
| Distance (in.) | Angle (°) | Power (amps) | Pressure (psi) | Y1 | Y2 | Y3 |
| 6 | 45 | 300 | 70 | 0.099 | 0.1228 | 0.1111 |
| 6 | 90 | 375 | 80 | 0.043 | 0.089 | 0.0625 |
| 6 | 67.5 | 450 | 90 | 0.04 | 0.0614 | 0.0443 |
| 12 | 45 | 375 | 90 | 0.128 | 0.137 | 0.1163 |
| 12 | 90 | 450 | 70 | 0.096 | 0.1183 | 0.1189 |
| 12 | 67.5 | 300 | 80 | 0.121 | 0.1169 | 0.0799 |
| 18 | 45 | 450 | 80 | 0.176 | 0.1641 | 0.1738 |
| 18 | 90 | 300 | 90 | 0.114 | 0.0955 | 0.54 |
| 18 | 67.5 | 375 | 70 | 0.138 | 0.1209 | 0.1497 |
| 12 | 90 | 375 | 80 | 0.078 | 0.0975 | 0.0971 |
| 12 | 90 | 375 | 80 | 0.076 | 0.1168 | 0.0875 |
| 12 | 90 | 375 | 80 | 0.091 | 0.0937 | 0.0648 |
| 12 | 90 | 375 | 80 | 0.111 | 0.0723 | 0.0605 |
| 12 | 90 | 375 | 80 | 0.104 | 0.0814 | 0.0931 |
| 12 | 90 | 375 | 80 | 0.104 | 0.0914 | 0.069 |
| 12 | 90 | 375 | 80 | 0.082 | 0.0854 | 0.0915 |
| 12 | 90 | 375 | 80 | 0.094 | 0.0815 | 0.1047 |
| 12 | 90 | 375 | 80 | 0.065 | 0.0771 | 0.0527 |
| 12 | 90 | 375 | 80 | 0.088 | 0.0536 | 0.0592 |
| 12 | 90 | 375 | 80 | 0.093 | 0.0515 | 0.0931 |
| 12 | 90 | 375 | 80 | 0.094 | 0.0714 | 0.0987 |

**Table C4. Cavitation erosion weight losses for Zn:Al (85:15) pseudo alloy**

| Settings | | | | Weight Loss/g | | |
|---|---|---|---|---|---|---|
| Distance (in.) | Angle (°) | Power (amps) | Pressure (psi) | Y1 | Y2 | Y3 |
| 6 | 45 | 300 | 70 | 0.068 | 0.0514 | 0.0763 |
| 6 | 90 | 375 | 80 | 0.045 | 0.0468 | 0.0522 |
| 6 | 67.5 | 450 | 90 | 0.048 | 0.0407 | 0.0693 |
| 12 | 45 | 375 | 90 | 0.053 | 0.0653 | 0.0944 |
| 12 | 90 | 450 | 70 | 0.067 | 0.0552 | 0.0645 |
| 12 | 67.5 | 300 | 80 | 0.083 | 0.0919 | 0.0694 |
| 18 | 45 | 450 | 80 | 0.072 | 0.1121 | 0.0695 |
| 18 | 90 | 300 | 90 | 0.064 | 0.0624 | 0.0916 |
| 18 | 67.5 | 375 | 70 | 0.097 | 0.085 | 0.0644 |
| 12 | 90 | 375 | 80 | 0.061 | 0.06 | 0.0544 |
| 12 | 90 | 375 | 80 | 0.049 | 0.0513 | 0.0583 |
| 12 | 90 | 375 | 80 | 0.048 | 0.0587 | 0.0572 |
| 12 | 90 | 375 | 80 | 0.069 | 0.0505 | 0.0501 |
| 12 | 90 | 375 | 80 | 0.039 | 0.0364 | 0.0444 |
| 12 | 90 | 375 | 80 | 0.046 | 0.0715 | 0.0633 |
| 12 | 90 | 375 | 80 | 0.043 | 0.0632 | 0.074 |
| 12 | 90 | 375 | 80 | 0.057 | 0.0469 | 0.0548 |
| 12 | 90 | 375 | 80 | 0.07 | 0.0422 | 0.0586 |
| 12 | 90 | 375 | 80 | 0.058 | 0.0599 | 0.0588 |
| 12 | 90 | 375 | 80 | 0.079 | 0.0579 | 0.071 |
| 12 | 90 | 375 | 80 | 0.07 | 0.0565 | 0.0614 |

**Table C5. Cavitation erosion weight losses for Al:$AlO_2$ (90:10) alloy.**

| Settings | | | | Weight Loss/g | | |
|---|---|---|---|---|---|---|
| Distance (in.) | Angle (°) | Power (amps) | Pressure (psi) | Y1 | Y2 | Y3 |
| 6 | 45 | 300 | 70 | 0.038 | 0.0379 | 0.0373 |
| 6 | 90 | 375 | 80 | 0.031 | 0.028 | 0.0258 |
| 6 | 67.5 | 450 | 90 | 0.031 | 0.0281 | 0.0284 |
| 12 | 45 | 375 | 90 | 0.038 | 0.0398 | 0.0389 |
| 12 | 90 | 450 | 70 | 0.056 | 0.0566 | 0.0544 |
| 12 | 67.5 | 300 | 80 | 0.049 | 0.0433 | 0.0459 |
| 18 | 45 | 450 | 80 | 0.038 | 0.036 | 0.0348 |
| 18 | 90 | 300 | 90 | 0.042 | 0.047 | 0.0451 |
| 18 | 67.5 | 375 | 70 | 0.048 | 0.047 | 0.0495 |
| 12 | 90 | 375 | 80 | 0.052 | 0.0526 | 0.0508 |
| 12 | 90 | 375 | 80 | 0.048 | 0.0478 | 0.0483 |
| 12 | 90 | 375 | 80 | 0.053 | 0.0584 | 0.0517 |
| 12 | 90 | 375 | 80 | 0.054 | 0.0555 | 0.0524 |
| 12 | 90 | 375 | 80 | 0.052 | 0.0489 | 0.0573 |
| 12 | 90 | 375 | 80 | 0.471 | 0.0547 | 0.0517 |
| 12 | 90 | 375 | 80 | 0.052 | 0.053 | 0.0524 |
| 12 | 90 | 375 | 80 | 0.053 | 0.0505 | 0.0491 |
| 12 | 90 | 375 | 80 | 0.472 | 0.4702 | 0.4816 |
| 12 | 90 | 375 | 80 | 0.47 | 0.4774 | 0.4747 |
| 12 | 90 | 375 | 80 | 0.477 | 0.4719 | 0.4762 |
| 12 | 90 | 375 | 80 | 0.475 | 0.4771 | 0.4736 |

# Appendix D: Porosity and Oxide Content Results

Tables D1 through D5 list the results of the image analysis in terms of proportion of pore and oxide versus metal for each film sample.

**Table D1. Porosity and oxide content for Zn:Al (85:15) alloy.**

| Sample Number | B&W1 | B&W2 | B&W3 |
|---|---|---|---|
| 1 | 0.09 | 0.08 | 0.07 |
| 2 | 0.09 | 0.05 | 0.04 |
| 3 | 0.07 | 0.05 | 0.06 |
| 4 | 0.14 | 0.14 | 0.12 |
| 5 | 0.11 | 0.07 | 0.1 |
| 6 | 0.09 | 0.09 | 0.08 |
| 7 | 0.24 | 0.12 | 0.16 |
| 8 | 0.05 | 0.09 | 0.08 |
| 9 | 0.12 | 0.12 | 0.09 |
| 10 | 0.09 | 0.1 | 0.09 |
| 11 | 0.07 | 0.09 | 0.1 |
| 12 | 0.11 | 0.09 | 0.16 |
| 13 | 0.05 | 0.06 | 0.05 |
| 14 | 0.09 | 0.07 | 0.11 |
| 15 | 0.1 | 0.06 | 0.09 |
| 16 | 0.06 | 0.09 | 0.1 |
| 17 | 0.09 | 0.08 | 0.07 |
| 18 | 0.14 | 0.08 | 0.1 |
| 19 | 0.1 | 0.09 | 0.09 |
| 20 | 0.08 | 0.09 | 0.1 |
| 21 | 0.09 | 0.07 | 0.1 |

**Table D2. Porosity and oxide content for Al.**

| Sample Number | B&W1 | B&W2 | B&W3 |
|---|---|---|---|
| 22 | 0.16 | 0.14 | 0.14 |
| 23 | 0.15 | 0.14 | 0.11 |
| 24 | 0.14 | 0.17 | 0.12 |
| 25 | 0.12 | 0.15 | 0.12 |
| 26 | 0.14 | 0.13 | 0.15 |
| 27 | 0.14 | 0.17 | 0.16 |
| 28 | 0.16 | 0.14 | 0.19 |
| 29 | 0.14 | 0.11 | 0.11 |
| 30 | 0.16 | 0.13 | 0.17 |
| 31 | 0.08 | 0.12 | 0.09 |
| 32 | 0.08 | 0.1 | 0.15 |
| 33 | 0.12 | 0.14 | 0.11 |
| 34 | 0.15 | 0.16 | 0.11 |
| 35 | 0.09 | 0.09 | 0.1 |
| 36 | 0.21 | 0.14 | 0.11 |
| 37 | 0.12 | 0.11 | 0.16 |
| 38 | 0.08 | 0.07 | 0.08 |
| 39 | 0.08 | 0.05 | 0.1 |
| 40 | 0.08 | 0.1 | 0.1 |
| 41 | 0.07 | 0.08 | 0.13 |
| 42 | 0.08 | 0.09 | 0.08 |

**Table D3. Porosity and oxide content for Zn.**

| Sample Number | B&W1 | B&W2 | B&W3 |
|---|---|---|---|
| 43 | 0.12 | 0.11 | 0.11 |
| 44 | 0.07 | 0.09 | 0.04 |
| 45 | 0.08 | 0.08 | 0.07 |
| 46 | 0.12 | 0.15 | 0.12 |
| 47 | 0.11 | 0.07 | 0.07 |
| 48 | 0.15 | 0.09 | 0.1 |
| 49 | 0.12 | 0.18 | 0.22 |
| 50 | 0.08 | 0.07 | 0.12 |
| 51 | 0.09 | 0.15 | 0.13 |
| 52 | 0.07 | 0.07 | 0.12 |
| 53 | 0.08 | 0.13 | 0.11 |
| 54 | 0.09 | 0.07 | 0.11 |
| 55 | 0.08 | 0.09 | 0.07 |
| 56 | 0.08 | 0.06 | 0.09 |
| 57 | 0.08 | 0.06 | 0.1 |
| 58 | 0.08 | 0.13 | 0.11 |
| 59 | 0.1 | 0.08 | 0.08 |
| 60 | 0.06 | 0.09 | 0.09 |
| 61 | 0.09 | 0.13 | 0.13 |
| 62 | 0.11 | 0.11 | 0.14 |
| 63 | 0.1 | 0.12 | 0.11 |

**Table D4. Porosity and oxide content for Zn:Al (85:15) pseudo alloy**

| Sample Number | B&W1 | B&W2 | B&W3 |
|---|---|---|---|
| 64 | 0.21 | 0.23 | 0.21 |
| 65 | 0.19 | 0.18 | 0.16 |
| 66 | 0.17 | 0.2 | 0.16 |
| 67 | 0.2 | 0.2 | 0.16 |
| 68 | 0.21 | 0.18 | 0.15 |
| 69 | 0.17 | 0.16 | 0.19 |
| 70 | 0.17 | 0.24 | 0.21 |
| 71 | 0.25 | 0.17 | 0.21 |
| 72 | 0.21 | 0.19 | 0.21 |
| 73 | 0.21 | 0.22 | 0.15 |
| 74 | 0.18 | 0.17 | 0.19 |
| 75 | 0.18 | 0.15 | 0.18 |
| 76 | 0.14 | 0.16 | 0.14 |
| 77 | 0.16 | 0.19 | 0.2 |
| 78 | 0.12 | 0.14 | 0.16 |
| 79 | 0.09 | 0.15 | 0.1 |
| 80 | 0.15 | 0.18 | 0.13 |
| 81 | 0.12 | 0.13 | 0.13 |
| 82 | 0.18 | 0.2 | 0.16 |
| 83 | 0.14 | 0.12 | 0.14 |
| 84 | 0.21 | 0.13 | 0.13 |

**Table D5 - Porosity and oxide content for Al:$AlO_2$ (90:10) alloy.**

| Sample Number | B&W1 | B&W2 | B&W3 |
|---|---|---|---|
| 85 | 0.36 | 0.3 | 0.28 |
| 86 | 0.1 | 0.11 | 0.17 |
| 87 | 0.27 | 0.2 | 0.3 |
| 88 | 0.17 | 0.23 | 0.26 |
| 89 | 0.22 | 0.31 | 0.23 |
| 90 | 0.23 | 0.26 | 0.23 |
| 91 | 0.28 | 0.22 | 0.17 |
| 92 | 0.24 | 0.22 | 0.16 |
| 93 | 0.55 | 0.16 | 0.27 |
| 94 | 0.28 | 0.19 | 0.26 |
| 95 | 0.19 | 0.22 | 0.23 |
| 96 | 0.22 | 0.2 | 0.25 |
| 97 | 0.27 | 0.27 | 0.28 |
| 98 | 0.25 | 0.26 | 0.27 |
| 99 | 0.2 | 0.21 | 0.28 |
| 100 | 0.2 | 0.24 | 0.3 |
| 101 | 0.15 | 0.34 | 0.21 |
| 102 | 0.2 | 0.22 | 0.17 |
| 103 | 0.23 | 0.18 | 0.22 |
| 104 | 0.23 | 0.2 | 0.26 |
| 105 | 0.27 | 0.24 | 0.28 |

# Appendix E: Summary Statistics

The following sections are the descriptive statistics for each of the primary data sets. These data sets include dry-film thickness readings, adhesion pull-off strength results, erosion weight loss results, and porosity and oxide content.

## Definitions for Standard Statistical Terms and Parameters Computed

The following standard statistical measures were computed for all quantitative data:

- Mean: The arithmetic average of all data points.
- Standard Error: A display of the means and upper and lower confidence intervals based on the standard error for subsets of one column "broken down" by group codes in another column.
- Median: The middle observation in a sample of ranked data. Most commonly used measure of central tendency with ordinal data. The median is the basis for comparison within several nonparametric statistics.
- Mode: The dominant value for the variable.
- Standard Deviation: A measure of the spread in the variance of the sample, given by the square root of the variance.
- Sample Variance: The average of the squared deviations of the measurements about their mean. This statistic gives an indication of the variability of a given sample or population. The square of the standard deviation is used in the development of a number of additional statistics.
- Kurtosis: Measures the flatness of a distribution or the heaviness of its tails. The standard is the normal distribution with a value of 0. Distributions with short tails have negative kurtosis, while distributions with a lot of extreme values have positive kurtosis. This measure may be obtained for either populations or samples.
- Skewness: Measures whether the values in a column are symmetric about the mean. Positive values indicate that the variable is skewed to the right, while negative values indicate that the variable is skewed to the left.
- Range: The span from highest to lowest value.
- Minimum: The lowest value.
- Maximum: The highest value.

- Sum: The total of all data points.
- Count: The total number of all data points.
- Confidence Level (95.0 percent): A display of means and their 95 and 99 percent confidence intervals for subsets of one column "broken down" by group codes in another column. These confidence intervals are calculated using the standard deviation of each separate subgroup, rather than a pooled standard deviation.

Simple correlation was also done between ordered pairs of results from the performance characteristics. This is useful in giving a picture of whether one characteristic (like porosity) has an influence on another (say, erosion resistance). The results from this regression analysis were discussed earlier (beginning on page 54).

## Dry-Film Thickness Measurements — Descriptive Statistics

The descriptive statistics for the dry-film thickness measurements made on each set of materials are provided in Tables E1 through E6. The data are shown for all samples (Table E1), then for each of the individual materials (Tables E2 – E6).

**Table E1. Descriptive statistics for DFT of main samples.**

| | DFT Average | DFT Low | DFT High |
|---|---|---|---|
| | | | |
| **Mean** | 13.8608 | 12.6024 | 15.5344 |
| **Standard Error** | 0.21178168 | 0.23212473 | 0.17250004 |
| **Median** | 14.7 | 13.6 | 16 |
| **Mode** | 15.7 | 15.1 | 16.8 |
| **Standard Deviation** | 2.36779113 | 2.59523335 | 1.92860906 |
| **Sample Variance** | 5.60643484 | 6.73523613 | 3.7195329 |
| **Kurtosis** | -0.9541446 | -1.0952181 | -0.2379191 |
| **Skewness** | -0.4395394 | -0.4383623 | -0.5740625 |
| **Range** | 9.9 | 10.3 | 9.3 |
| **Minimum** | 8.5 | 6.9 | 10 |
| **Maximum** | 18.4 | 17.2 | 19.3 |
| **Sum** | 1732.6 | 1575.3 | 1941.8 |
| **Count** | 125 | 125 | 125 |
| **Confidence Level (95.0%)** | 0.41917497 | 0.45943954 | 0.34142566 |

**Table E2. Descriptive statistics for DFT readings from Zn:Al (85:15) alloy.**

| | DFT Average | DFT Low | DFT High |
|---|---|---|---|
| | | | |
| **Mean** | 10.9809524 | 9.2952381 | 13.6714286 |
| **Standard Error** | 0.27208359 | 0.26163189 | 0.32748267 |
| **Median** | 11.2 | 9.5 | 13.7 |
| **Mode** | 11.9 | 9.5 | 14.8 |
| **Standard Deviation** | 1.24684363 | 1.19894795 | 1.50071412 |
| **Sample Variance** | 1.55461905 | 1.43747619 | 2.25214286 |
| **Kurtosis** | -0.1852416 | -0.2352722 | 0.99202876 |
| **Skewness** | -0.4491248 | -0.4816936 | -0.3087818 |
| **Range** | 4.6 | 4.6 | 6.8 |
| **Minimum** | 8.5 | 6.9 | 10 |
| **Maximum** | 13.1 | 11.5 | 16.8 |
| **Sum** | 230.6 | 195.2 | 287.1 |
| **Count** | 21 | 21 | 21 |
| **Confidence Level (95.0%)** | 0.56755615 | 0.54575431 | 0.68311656 |

**Table E3. Descriptive statistics for DFT readings from Al.**

| DFT Average | DFT Average | DFT Low | DFT High |
|---|---|---|---|
| | | | |
| **Mean** | 11.2047619 | 9.78571429 | 13.3047619 |
| **Standard Error** | 0.23659048 | 0.24135389 | 0.27224605 |
| **Median** | 11.5 | 10.3 | 13.3 |
| **Mode** | 11.5 | 10.6 | 13.3 |
| **Standard Deviation** | 1.0841938 | 1.10602247 | 1.24758815 |
| **Sample Variance** | 1.17547619 | 1.22328571 | 1.55647619 |
| **Kurtosis** | -0.1770439 | -0.0909711 | 1.87264934 |
| **Skewness** | -0.8314708 | -1.0662467 | -0.7813663 |
| **Range** | 3.9 | 3.8 | 5.8 |
| **Minimum** | 8.7 | 7.2 | 10 |
| **Maximum** | 12.6 | 11 | 15.8 |
| **Sum** | 235.3 | 205.5 | 279.4 |
| **Count** | 21 | 21 | 21 |
| **Confidence Level (95.0%)** | 0.49351887 | 0.50345516 | 0.56789505 |

**Table E4. Descriptive statistics for DFT readings from Zn.**

| | DFT Average | DFT Low | DFT High |
|---|---|---|---|
| | | | |
| **Mean** | 15.7952381 | 14.5190476 | 17.0952381 |
| **Standard Error** | 0.19029754 | 0.17749836 | 0.21173616 |
| **Median** | 16.2 | 14.8 | 17.3 |
| **Mode** | 16.3 | 15.1 | 17.6 |
| **Standard Deviation** | 0.87205286 | 0.81339969 | 0.97029696 |
| **Sample Variance** | 0.76047619 | 0.66161905 | 0.94147619 |
| **Kurtosis** | -0.3350107 | -0.8041073 | 0.29276471 |
| **Skewness** | -1.079948 | -0.7968951 | -0.8759723 |
| **Range** | 2.8 | 2.5 | 3.8 |
| **Minimum** | 14 | 13 | 14.8 |
| **Maximum** | 16.8 | 15.5 | 18.6 |
| **Sum** | 331.7 | 304.9 | 359 |
| **Count** | 21 | 21 | 21 |
| **Confidence Level (95.0%)** | 0.39695352 | 0.37025493 | 0.44167368 |

**Table E5. Descriptive statistics for DFT readings from Zn:Al (85:15) pseudo alloy.**

| | DFT Average | DFT Low | DFT High |
|---|---|---|---|
| | | | |
| **Mean** | 15.4952381 | 14.4571429 | 16.9571429 |
| **Standard Error** | 0.19621128 | 0.21298015 | 0.17829502 |
| **Median** | 15.5 | 14.5 | 16.8 |
| **Mode** | 16.4 | 13.6 | 17.5 |
| **Standard Deviation** | 0.89915304 | 0.97599766 | 0.81705044 |
| **Sample Variance** | 0.80847619 | 0.95257143 | 0.66757143 |
| **Kurtosis** | 2.83228711 | 1.72532351 | 0.00490245 |
| **Skewness** | 1.2134504 | 0.88092952 | 0.436406 |
| **Range** | 3.9 | 4.4 | 3.2 |
| **Minimum** | 14.3 | 12.8 | 15.5 |
| **Maximum** | 18.2 | 17.2 | 18.7 |
| **Sum** | 325.4 | 303.6 | 356.1 |
| **Count** | 21 | 21 | 21 |
| **Confidence Level (95.0%)** | 0.40928937 | 0.4442686 | 0.37191673 |

**Table E6. Descriptive statistics for DFT readings from Al:$AlO_2$ (90:10) alloy.**

| | DFT Average | DFT Low | DFT High |
|---|---|---|---|
| | | | |
| **Mean** | 10.9809524 | 9.2952381 | 13.6714286 |
| **Standard Error** | 0.27208359 | 0.26163189 | 0.32748267 |
| **Median** | 11.2 | 9.5 | 13.7 |
| **Mode** | 11.9 | 9.5 | 14.8 |
| **Standard Deviation** | 1.24684363 | 1.19894795 | 1.50071412 |
| **Sample Variance** | 1.55461905 | 1.43747619 | 2.25214286 |
| **Kurtosis** | -0.1852416 | -0.2352722 | 0.99202876 |
| **Skewness** | -0.4491248 | -0.4816936 | -0.3087818 |
| **Range** | 4.6 | 4.6 | 6.8 |
| **Minimum** | 8.5 | 6.9 | 10 |
| **Maximum** | 13.1 | 11.5 | 16.8 |
| **Sum** | 230.6 | 195.2 | 287.1 |
| **Count** | 21 | 21 | 21 |
| **Confidence Level (95.0%)** | 0.56755615 | 0.54575431 | 0.68311656 |

## Descriptive Statistics for Adhesion Results

Descriptive statistics of the average pull-off adhesion measurements obtained from five pull-off tests performed on each of the 105 thermal spray coating samples are given in Table E7.

**Table E7. Descriptive statistics for adhesion pull-off strength (all materials).**

| Average Adhesion | Material 1 Zn:Al (85:15) | Material 2 Aluminum | Material 3 Zinc | Material 4 Zn:Al (85:15) Pseudo | Material 5 Al:$AlO_2$ (90:10) |
|---|---|---|---|---|---|
| | | | | | |
| **Mean** | 1167.68 | 1836.47 | 853.95 | 1372.30 | 1945.60 |
| **Standard Error** | 28.46 | 50.21 | 26.87 | 16.23 | 39.06 |
| **Median** | 1149.2 | 1851.2 | 819.48 | 1365.6 | 1931.4 |
| **Mode** | 1206.2 | 1580.6 | 876.04 | 1410.4 | 1997 |
| **Standard Deviation** | 130.42 | 230.08 | 123.14 | 74.38 | 179.02 |
| **Sample Variance** | 17008.14 | 52934.60 | 15162.99 | 5531.66 | 32047.16 |
| **Kurtosis** | 2.40 | 0.25 | 2.50 | 2.42 | 0.18 |
| **Skewness** | 1.37 | 0.43 | 1.72 | 1.10 | 0.65 |
| **Range** | 555.12 | 898 | 448.02 | 331.4 | 702.2 |
| **Minimum** | 993.88 | 1458 | 737.78 | 1255.4 | 1678.4 |
| **Maximum** | 1549 | 2356 | 1185.8 | 1586.8 | 2380.6 |
| **Sum** | 24521.34 | 38565.82 | 17933 | 28818.2 | 40857.68 |
| **Count** | 21 | 21 | 21 | 21 | 21 |
| **Confidence Level (95.0%)** | 59.36 | 104.73 | 56.05 | 33.86 | 81.49 |

## Descriptive Statistics for Erosion Measurements

The descriptive statistics for the average of the cavitation erosion weight losses suffered by three replicate specimens for each of the thermal spray samples are shown in Table E8. The statistics are grouped by material type.

**Table E8. Descriptive statistics for erosion weight losses.**

| Average Erosion | Material 1 Zn:Al (85:15) | Material 2 Aluminum | Material 3 Zinc | Material 4 Zn:Al (85:15) Pseudo | Material 5 Al:$AlO_2$ (90:10) |
|---|---|---|---|---|---|
| | | | | | |
| **Mean** | 0.055 | 0.045 | 0.102 | 0.062 | 0.134 |
| **Standard Error** | 0.010 | 0.002 | 0.009 | 0.002 | 0.038 |
| **Median** | 0.043 | 0.049 | 0.091 | 0.060 | 0.052 |
| **Mode** | ... | ... | ... | ... | ... |
| **Standard Deviation** | 0.044 | 0.008 | 0.043 | 0.011 | 0.172 |
| **Sample Variance** | 0.002 | 0.000 | 0.002 | 0.000 | 0.030 |
| **Kurtosis** | 7.186 | -0.735 | 6.373 | -0.031 | 0.684 |
| **Skewness** | 2.876 | -0.733 | 2.240 | 0.452 | 1.581 |
| **Range** | 0.156 | 0.026 | 0.201 | 0.044 | 0.447 |
| **Minimum** | 0.030 | 0.030 | 0.049 | 0.040 | 0.028 |
| **Maximum** | 0.186 | 0.056 | 0.250 | 0.084 | 0.475 |
| **Sum** | 1.162 | 0.953 | 2.133 | 1.303 | 2.820 |
| **Count** | 21 | 21 | 21 | 21 | 21 |
| **Confidence Level (95.0%)** | 0.02) | 0.00) | 0.02) | 0.01) | 0.08) |

## Porosity and Oxide Content - Image Analysis Descriptive Statistics

The descriptive statistics for the porosity and oxide content, grouped by material type, are given in Table E9.

**Table E9. Descriptive statistics for porosity and oxide content (all materials).**

| Average Porosity Oxide | Material 1 Zn:Al (85:15) | Material 2 Aluminum | Material 3 Zinc | Material 4 Zn:Al (85:15) Pseudo | Material 5 Al:$AlO_2$ (90:10) |
|---|---|---|---|---|---|
| | | | | | |
| **Mean** | 0.092 | 0.122 | 0.100 | 0.172 | 0.238 |
| **Standard Error** | 0.006 | 0.006 | 0.005 | 0.006 | 0.009 |
| **Median** | 0.087 | 0.130 | 0.090 | 0.177 | 0.233 |
| **Mode** | 0.093 | 0.093 | 0.080 | 0.180 | 0.223 |
| **Standard Deviation** | 0.027 | 0.028 | 0.025 | 0.028 | 0.041 |
| **Sample Variance** | 0.001 | 0.001 | 0.001 | 0.001 | 0.002 |
| **Kurtosis** | 3.517 | -1.303 | 2.258 | -0.462 | 2.449 |
| **Skewness** | 1.466 | -0.272 | 1.228 | -0.413 | -0.226 |
| **Range** | 0.120 | 0.087 | 0.107 | 0.103 | 0.200 |
| **Minimum** | 0.053 | 0.077 | 0.067 | 0.113 | 0.127 |
| **Maximum** | 0.173 | 0.163 | 0.173 | 0.217 | 0.327 |
| **Sum** | 1.937 | 2.557 | 2.110 | 3.607 | 4.990 |
| **Count** | 21 | 21 | 21 | 21 | 21 |
| **Confidence Level (95.0%)** | 0.012 | 0.013 | 0.011 | 0.013 | 0.019 |

## Descriptive Statistics for Outer Arrays — Center-Point Samples

The descriptive statistics for the outer array center-point samples are provided on the following pages.

| Descriptive Estimates for Material 1 Average Adhesion | | | |
|---|---|---|---|
| Sample Size | 12 | Minimum | 1051.3 |
| Number Missing | 0 | Maximum | 1271.2 |
| Sum | 13608.7998 | Range | 219.8999 |
| Sum of Squares | 15482129.92 | Semi-Inner Qt. Range | 57.3 |
| Mean | 1134.0667 | Median | 1116.2999 |
| Lower 99% C.I. | 1074.323 | 5th Percentile | 1051.3 |
| Lower 95% C.I. | 1091.7279 | 10th Percentile | 1051.3 |
| Upper 95% C.I. | 1176.4054 | 25th Percentile | 1091.6 |
| Upper 99% C.I. | 1193.8103 | 75th Percentile | 1206.2 |
| Adj. Sum Squares | 48843.9127 | 90th Percentile | 1271.2 |
| Harmonic Mean | 1130.6031 | 95th Percentile | 1271.2 |
| Variance | 4440.3557 | Standard Error; | 19.2362 |
| Standard Deviation | 66.636 | t-Value (Mean=0) | 58.955 |
| Coef. of Variation | 0.0588 | Mean Abs. Dev | 53.2778 |
| Skewness | 0.8061 | Kurtosis | -0.0143 |

| Descriptive Estimates for Material 1 Average Erosion | | | |
|---|---|---|---|
| Sample Size | 12 | Minimum | 0.0297 |
| Number Missing | 0 | Maximum | 0.1841 |
| Sum | 0.6381 | Range | 0.1545 |
| Sum of Squares | 0.0531 | Semi-Inner Qt. Range | 0.0053 |
| Mean | 0.0532 | Median | 0.0439 |
| Lower 99% C.I. | 0.0158 | 5th Percentile | 0.0297 |
| Lower 95% C.I. | 0.0267 | 10th Percentile | 0.0297 |
| Upper 95% C.I. | 0.0797 | 25th Percentile | 0.0365 |
| Upper 99% C.I. | 0.0906 | 75th Percentile | 0.0471 |
| Adj. Sum Squares | 0.0191 | 90th Percentile | 0.1841 |
| Harmonic Mean | 0.043 | 95th Percentile | 0.1841 |
| Variance | 0.0017 | Standard Error; | 0.012 |
| Standard Deviation | 0.0417 | t-Value (Mean=0) | 4.4165 |
| Coef. of Variation | 0.7844 | Mean Abs. Dev | 0.0218 |
| Skewness | 3.3235 | Kurtosis | 11.3186 |

| Descriptive Estimates for Material 1 Average Porosity Oxide | | | |
|---|---|---|---|
| Sample Size | 12 | Minimum | 0.0533 |
| Number Missing | 0 | Maximum | 0.12 |
| Sum | 1.0667 | Range | 0.0667 |
| Sum of Squares | 0.0976 | Semi-Inner Qt. Range | 0.005 |
| Mean | 0.0889 | Median | 0.0883 |
| Lower 99% C.I. | 0.0747 | 5th Percentile | 0.0533 |
| Lower 95% C.I. | 0.0789 | 10th Percentile | 0.0533 |
| Upper 95% C.I. | 0.0989 | 25th Percentile | 0.0833 |
| Upper 99% C.I. | 0.103 | 75th Percentile | 0.0933 |
| Adj. Sum Squares | 0.0027 | 90th Percentile | 0.12 |
| Harmonic Mean | 0.0859 | 95th Percentile | 0.12 |
| Variance | 0.0002 | Standard Error; | 0.0046 |
| Standard Deviation | 0.0158 | t-Value (Mean=0) | 19.5074 |
| Coef. of Variation | 0.1776 | Mean Abs. Dev | 0.01 |
| Skewness | -0.2803 | Kurtosis | 2.6776 |

| Descriptive Estimates for Material 2 Average Adhesion | | | |
|---|---|---|---|
| Sample Size | 12 | Minimum | 1482.62 |
| Number Missing | 0 | Maximum | 1924.6 |
| Sum | 21135.4199 | Range | 441.98 |
| Sum of Squares | 37444193.95 | Semi-Inner Qt. Range | 135.2 |
| Mean | 1761.285 | Median | 1796.1 |
| Lower 99% C.I. | 1634.8676 | 5th Percentile | 1482.62 |
| Lower 95% C.I. | 1671.6962 | 10th Percentile | 1482.62 |
| Upper 95% C.I. | 1850.8737 | 25th Percentile | 1629.6 |
| Upper 99% C.I. | 1887.7024 | 75th Percentile | 1900 |
| Adj. Sum Squares | 218696.0148 | 90th Percentile | 1924.6 |
| Harmonic Mean | 1750.3495 | 95th Percentile | 1924.6 |
| Variance | 19881.4559 | Standard Error; | 40.7037 |
| Standard Deviation | 141.0016 | t-Value (Mean=0) | 43.2709 |
| Coef. of Variation | 0.0801 | Mean Abs. Dev | 114.3675 |
| Skewness | -0.7238 | Kurtosis | -0.392 |

| Descriptive Estimates for Material 2 Average Erosion | | | |
|---|---|---|---|
| Sample Size | 12 | Minimum | 0.0465 |
| Number Missing | 0 | Maximum | 0.0559 |
| Sum | 0.6162 | Range | 0.0094 |
| Sum of Squares | 0.0317 | Semi-Inner Qt. Range | 0.0016 |
| Mean | 0.0514 | Median | 0.0512 |
| Lower 99% C.I. | 0.0492 | 5th Percentile | 0.0465 |
| Lower 95% C.I. | 0.0498 | 10th Percentile | 0.0465 |
| Upper 95% C.I. | 0.0529 | 25th Percentile | 0.0499 |
| Upper 99% C.I. | 0.0535 | 75th Percentile | 0.0531 |
| Adj. Sum Squares | 0.0001 | 90th Percentile | 0.0559 |
| Harmonic Mean | 0.0512 | 95th Percentile | 0.0559 |
| Variance | 0 | Standard Error; | 0.0007 |
| Standard Deviation | 0.0024 | t-Value (Mean=0) | 74.2496 |
| Coef. of Variation | 0.0467 | Mean Abs. Dev | 0.0018 |
| Skewness | -0.134 | Kurtosis | 0.941 |

| Descriptive Estimates for Material 2 Average Porosity Oxide | | | |
|---|---|---|---|
| Sample Size | 12 | Minimum | 0.0767 |
| Number Missing | 0 | Maximum | 0.1533 |
| Sum | 1.27 | Range | 0.0767 |
| Sum of Squares | 0.1415 | Semi-Inner Qt. Range | 0.0233 |
| Mean | 0.1058 | Median | 0.095 |
| Lower 99% C.I. | 0.0831 | 5th Percentile | 0.0767 |
| Lower 95% C.I. | 0.0897 | 10th Percentile | 0.0767 |
| Upper 95% C.I. | 0.122 | 25th Percentile | 0.0833 |
| Upper 99% C.I. | 0.1286 | 75th Percentile | 0.13 |
| Adj. Sum Squares | 0.0071 | 90th Percentile | 0.1533 |
| Harmonic Mean | 0.1007 | 95th Percentile | 0.1533 |
| Variance | 0.0006 | Standard Error; | 0.0073 |
| Standard Deviation | 0.0254 | t-Value (Mean=0) | 14.4389 |
| Coef. of Variation | 0.2399 | Mean Abs. Dev | 0.0213 |
| Skewness | 0.6595 | Kurtosis | -0.7454 |

| Descriptive Estimates for Material 3 Average Adhesion | | | |
|---|---|---|---|
| Sample Size | 12 | Minimum | 737.78 |
| Number Missing | 0 | Maximum | 876.04 |
| Sum | 9633.7199 | Range | 138.2599 |
| Sum of Squares | 7759749.224 | Semi-Inner Qt. Range | 43.59 |
| Mean | 802.81 | Median | 792.92 |
| Lower 99% C.I. | 759.4714 | 5th Percentile | 737.78 |
| Lower 95% C.I. | 772.097 | 10th Percentile | 737.78 |
| Upper 95% C.I. | 833.523 | 25th Percentile | 764.36 |
| Upper 99% C.I. | 846.1486 | 75th Percentile | 851.54 |
| Adj. Sum Squares | 25702.6156 | 90th Percentile | 876.04 |
| Harmonic Mean | 800.1738 | 95th Percentile | 876.04 |
| Variance | 2336.6014 | Standard Error; | 13.9541 |
| Standard Deviation | 48.3384 | t-Value (Mean=0) | 57.5322 |
| Coef. of Variation | 0.0602 | Mean Abs. Dev | 40.125 |
| Skewness | 0.2914 | Kurtosis | -1.12 |

| Descriptive Estimates for Material 3 Average Erosion | | | |
|---|---|---|---|
| Sample Size | 12 | Minimum | 0.065 |
| Number Missing | 0 | Maximum | 0.0934 |
| Sum | 1.0078 | Range | 0.0283 |
| Sum of Squares | 0.0857 | Semi-Inner Qt. Range | 0.0067 |
| Mean | 0.084 | Median | 0.087 |
| Lower 99% C.I. | 0.0754 | 5th Percentile | 0.065 |
| Lower 95% C.I. | 0.0779 | 10th Percentile | 0.065 |
| Upper 95% C.I. | 0.0901 | 25th Percentile | 0.0793 |
| Upper 99% C.I. | 0.0926 | 75th Percentile | 0.0928 |
| Adj. Sum Squares | 0.001 | 90th Percentile | 0.0934 |
| Harmonic Mean | 0.0828 | 95th Percentile | 0.0934 |
| Variance | 0.0001 | Standard Error; | 0.0028 |
| Standard Deviation | 0.0096 | t-Value (Mean=0) | 30.2574 |
| Coef. of Variation | 0.1145 | Mean Abs. Dev | 0.0074 |
| Skewness | -1.1323 | Kurtosis | 0.3866 |

| Descriptive Estimates for Material 3 Average Porosity Oxide | | | |
|---|---|---|---|
| Sample Size | 12 | Minimum | 0.0767 |
| Number Missing | 0 | Maximum | 0.12 |
| Sum | 1.14 | Range | 0.0433 |
| Sum of Squares | 0.1111 | Semi-Inner Qt. Range | 0.015 |
| Mean | 0.095 | Median | 0.0883 |
| Lower 99% C.I. | 0.0808 | 5th Percentile | 0.0767 |
| Lower 95% C.I. | 0.0849 | 10th Percentile | 0.0767 |
| Upper 95% C.I. | 0.1051 | 25th Percentile | 0.08 |
| Upper 99% C.I. | 0.1092 | 75th Percentile | 0.11 |
| Adj. Sum Squares | 0.0028 | 90th Percentile | 0.12 |
| Harmonic Mean | 0.0927 | 95th Percentile | 0.12 |
| Variance | 0.0003 | Standard Error; | 0.0046 |
| Standard Deviation | 0.0159 | t-Value (Mean=0) | 20.7507 |
| Coef. of Variation | 0.1669 | Mean Abs. Dev | 0.0142 |
| Skewness | 0.4042 | Kurtosis | -1.6077 |

| Descriptive Estimates for Material 4 Average Adhesion | | | |
|---|---|---|---|
| Sample Size | 12 | Minimum | 1312.4 |
| Number Missing | 0 | Maximum | 1434.6 |
| Sum | 16348.6 | Range | 122.2 |
| Sum of Squares | 22287820.21 | Semi-Inner Qt. Range | 28.6 |
| Mean | 1362.3833 | Median | 1363.5 |
| Lower 99% C.I. | 1329.5412 | 5th Percentile | 1312.4 |
| Lower 95% C.I. | 1339.109 | 10th Percentile | 1312.4 |
| Upper 95% C.I. | 1385.6577 | 25th Percentile | 1324.6 |
| Upper 99% C.I. | 1395.2255 | 75th Percentile | 1381.8 |
| Adj. Sum Squares | 14760.1177 | 90th Percentile | 1434.6 |
| Harmonic Mean | 1361.4892 | 95th Percentile | 1434.6 |
| Variance | 1341.8289 | Standard Error; | 10.5745 |
| Standard Deviation | 36.631 | t-Value (Mean=0) | 128.8372 |
| Coef. of Variation | 0.0269 | Mean Abs. Dev | 27.55 |
| Skewness | 0.4732 | Kurtosis | -0.0422 |

| Descriptive Estimates for Material 4 Average Erosion | | | |
|---|---|---|---|
| Sample Size | 12 | Minimum | 0.0399 |
| Number Missing | 0 | Maximum | 0.0692 |
| Sum | 0.6832 | Range | 0.0293 |
| Sum of Squares | 0.0394 | Semi-Inner Qt. Range | 0.0038 |
| Mean | 0.0569 | Median | 0.0577 |
| Lower 99% C.I. | 0.0506 | 5th Percentile | 0.0399 |
| Lower 95% C.I. | 0.0525 | 10th Percentile | 0.0399 |
| Upper 95% C.I. | 0.0614 | 25th Percentile | 0.0528 |
| Upper 99% C.I. | 0.0632 | 75th Percentile | 0.0604 |
| Adj. Sum Squares | 0.0005 | 90th Percentile | 0.0692 |
| Harmonic Mean | 0.056 | 95th Percentile | 0.0692 |
| Variance | 0 | Standard Error; | 0.002 |
| Standard Deviation | 0.007 | t-Value (Mean=0) | 28.1378 |
| Coef. of Variation | 0.1231 | Mean Abs. Dev | 0.0047 |
| Skewness | -0.9332 | Kurtosis | 3.0388 |

| Descriptive Estimates for Material 4 Average Porosity Oxide | | | |
|---|---|---|---|
| Sample Size | 12 | Minimum | 0.1133 |
| Number Missing | 0 | Maximum | 0.1933 |
| Sum | 1.8767 | Range | 0.08 |
| Sum of Squares | 0.3005 | Semi-Inner Qt. Range | 0.0233 |
| Mean | 0.1564 | Median | 0.155 |
| Lower 99% C.I. | 0.1337 | 5th Percentile | 0.1133 |
| Lower 95% C.I. | 0.1403 | 10th Percentile | 0.1133 |
| Upper 95% C.I. | 0.1725 | 25th Percentile | 0.1333 |
| Upper 99% C.I. | 0.1791 | 75th Percentile | 0.18 |
| Adj. Sum Squares | 0.007 | 90th Percentile | 0.1933 |
| Harmonic Mean | 0.1525 | 95th Percentile | 0.1933 |
| Variance | 0.0006 | Standard Error; | 0.0073 |
| Standard Deviation | 0.0253 | t-Value (Mean=0) | 21.426 |
| Coef. of Variation | 0.1617 | Mean Abs. Dev | 0.0208 |
| Skewness | -0.1677 | Kurtosis | -1.093 |

| Descriptive Estimates for Material 5 Average Adhesion | | | |
|---|---|---|---|
| Sample Size | 12 | Minimum | 1678.4 |
| Number Missing | 0 | Maximum | 1997 |
| Sum | 22256.3999 | Range | 318.6 |
| Sum of Squares | 41386156.1 | Semi-Inner Qt. Range | 102 |
| Mean | 1854.7 | Median | 1858.1 |
| Lower 99% C.I. | 1766.187 | 5th Percentile | 1678.4 |
| Lower 95% C.I. | 1791.9731 | 10th Percentile | 1678.4 |
| Upper 95% C.I. | 1917.4268 | 25th Percentile | 1760.2 |
| Upper 99% C.I. | 1943.213 | 75th Percentile | 1964.2 |
| Adj. Sum Squares | 107211.3866 | 90th Percentile | 1997 |
| Harmonic Mean | 1849.8252 | 95th Percentile | 1997 |
| Variance | 9746.4897 | Standard Error; | 28.4993 |
| Standard Deviation | 98.7243 | t-Value (Mean=0) | 65.0789 |
| Coef. of Variation | 0.0532 | Mean Abs. Dev | 78.2 |
| Skewness | -0.2092 | Kurtosis | -0.8594 |

| Descriptive Estimates for Material 5 Average Erosion | | | |
|---|---|---|---|
| Sample Size | 7 | Minimum | 0.0482 |
| Number Missing | 0 | Maximum | 0.0544 |
| Sum | 0.3642 | Range | 0.0062 |
| Sum of Squares | 0.019 | Semi-Inner Qt. Range | 0.0015 |
| Mean | 0.052 | Median | 0.0524 |
| Lower 99% C.I. | 0.0491 | 5th Percentile | 0.0482 |
| Lower 95% C.I. | 0.0501 | 10th Percentile | 0.0482 |
| Upper 95% C.I. | 0.054 | 25th Percentile | 0.051 |
| Upper 99% C.I. | 0.055 | 75th Percentile | 0.054 |
| Adj. Sum Squares | 0 | 90th Percentile | 0.0544 |
| Harmonic Mean | 0.052 | 95th Percentile | 0.0544 |
| Variance | 0 | Standard Error; | 0.0008 |
| Standard Deviation | 0.0021 | t-Value (Mean=0) | 66.0486 |
| Coef. of Variation | 0.0401 | Mean Abs. Dev | 0.0015 |
| Skewness | -0.9762 | Kurtosis | 1.3038 |

| Descriptive Estimates for Material 5 Average Porosity Oxide | | | |
|---|---|---|---|
| Sample Size | 12 | Minimum | 0.1967 |
| Number Missing | 0 | Maximum | 0.2733 |
| Sum | 2.8233 | Range | 0.0767 |
| Sum of Squares | 0.6701 | Semi-Inner Qt. Range | 0.0233 |
| Mean | 0.2353 | Median | 0.2317 |
| Lower 99% C.I. | 0.2146 | 5th Percentile | 0.1967 |
| Lower 95% C.I. | 0.2206 | 10th Percentile | 0.1967 |
| Upper 95% C.I. | 0.2499 | 25th Percentile | 0.2133 |
| Upper 99% C.I. | 0.256 | 75th Percentile | 0.26 |
| Adj. Sum Squares | 0.0059 | 90th Percentile | 0.2733 |
| Harmonic Mean | 0.2332 | 95th Percentile | 0.2733 |
| Variance | 0.0005 | Standard Error; | 0.0067 |
| Standard Deviation | 0.0231 | t-Value (Mean=0) | 35.3279 |
| Coef. of Variation | 0.0981 | Mean Abs. Dev | 0.0184 |
| Skewness | 0.0712 | Kurtosis | -0.6979 |

## Distribution

Chief of Engineers
ATTN: CEHEC-IM-LH (2)
ATTN: CEHEC-IM-LP (2)
ATTN: CECC-R
ATTN: CERD-L
ATTN: CERD-M
ATTN: CECW-EE

Defense Tech Info Center 22304
ATTN: DTIC-O (2)

10
2/99